

Lithium Niobate on Insulator: An Emerging Platform for Integrated Quantum Photonics

Sina Saravi, Thomas Pertsch,* and Frank Setzpfandt*


Due to its properties, lithium niobate is one of the most suitable material platforms for the implementation of integrated optical quantum circuits. With the commercialization of lithium niobate on insulator (LNOI) substrates in the recent years, the lithium niobate nanostructuring technology has progressed immensely. Now nanostructured LNOI components can be fabricated with a quality on par with any other material platform, and could act as effective building blocks for integrated quantum circuits. The advanced nanostructuring technology combined with its favorable material properties make the LNOI platform a real contender for the realization of large-scale optical quantum circuits. The aim of this perspective article is to examine the utility of the LNOI platform toward this goal. To do this, first the availability of the individual components that can act as the building blocks for such circuits is investigated. Afterward, a fully on-chip implementation of a multiplexed source of single photons on the LNOI platform is envisioned, which is a highly challenging task in all material platforms. Based on the performance of the state-of-the-art components on the LNOI platform, the performance of such a device is quantified and the areas in which more progress is needed are pointed out.

1. Introduction

For the large-scale implementation of optical quantum information processing protocols^[1–3] requiring potentially hundreds of different functional optical elements, on-chip integration is inevitable.^[4] To date many different technologies and material platforms for integrated optics have been evaluated for this

S. Saravi, T. Pertsch, F. Setzpfandt
Institute of Applied Physics
Abbe Center of Photonics
Friedrich Schiller University Jena
Albert-Einstein-Str. 15, 07745 Jena, Germany
E-mail: thomas.pertsch@uni-jena.de; f.setzpfandt@uni-jena.de

T. Pertsch
Fraunhofer Institute for Applied Optics and Precision Engineering
Albert-Einstein-Str. 7, 07745 Jena, Germany

 The ORCID identification number(s) for the author(s) of this article can be found under <https://doi.org/10.1002/adom.202100789>.

© 2021 The Authors. Advanced Optical Materials published by Wiley-VCH GmbH. This is an open access article under the terms of the Creative Commons Attribution-NonCommercial License, which permits use, distribution and reproduction in any medium, provided the original work is properly cited and is not used for commercial purposes.

Correction added on 14 January 2022, after first online publication: Thomas Pertsch was designated as corresponding author.

DOI: 10.1002/adom.202100789

goal. Up to now, silicon photonics has been one of the workhorses of integrated optical quantum technologies^[5] due to its matured fabrication technology. However, from the point of view of relevant optical properties, silicon itself is not the most suitable material platform,^[6,7] as it suffers from two-photon absorption loss, which also makes the realization of fast and low-loss switches challenging.^[5]

Several alternative material platforms for integrated quantum photonics have been suggested.^[6,7] Among them, lithium niobate (LN) is recognized as a highly suitable candidate for implementing optical quantum circuitry. LN has many favorable properties, such as a large transparency window, strong second-order nonlinearity, possibility for periodic poling, and access to fast and low-loss switching through the electro-optic effect.^[8] LN has been used extensively for the integrated implementation of quantum optical protocols using indiffusion or proton exchange waveguide technologies

with weak mode confinement. However, a true large-scale implementation requires a high-density integration of compact and low-loss nanostructured components, requiring a dedicated fabrication technology on the LN platform, the development of which started only about a decade ago.^[9] In the last few years, with the commercial availability of lithium niobate on insulator (LNOI) substrates, there has been an enormous progress in the fabrication of nanostructured elements on the LNOI platform,^[10–13] such that state-of-the-art LNOI nanostructured elements have a quality on a par with current silicon photonics technology.^[5] This makes the LNOI platform a truly viable candidate for large-scale on-chip implementation of optical quantum protocols.

There have already been few very recent reviews on the development of nanostructured components on the LNOI platform.^[11–16] The specific objective of this progress report is to take a detailed look at these recent developments and to show, that lithium niobate is very suitable for large-scale integrated quantum optics. To do this, we split this report in two parts. In the first part we start describing in detail what makes the LNOI platform uniquely attractive for integrated quantum optical applications. We then review the functional elements available on the LNOI platform and categorize them in terms of the needed building blocks for integrated quantum optics. In the second part of this report we underscore the suitability of the LNOI platform for integrated quantum photonics by quantitatively evaluating the implementation of a multiplexed

single-photon source. This is a crucial missing component for a practical large-scale implementation of optical quantum computation and simulation protocols. Here we will argue that such a source could be implemented on the LNOI platform and quantify its potential performance based on the quality of the state-of-the-art nanostructuring technology demonstrated on LNOI. We also point out the areas in which technological developments are needed for a feasible realization and suggest future avenues of research for improving the performance of such a source. With this discussion we will show, that LNOI has large potential as a platform for integrated quantum photonics in general.

2. Implementation of Functional Quantum Photonic Elements on the LNOI Platform

Integrated quantum photonics is based on a number of specific functional building blocks that enable to generate, control, and detect tailored quantum light on photonic chips.^[4,7] As we will show below, the LNOI platform has the potential for realizing all of the necessary functional photonic elements and thus is ideally suited for integrated quantum photonics. Before we review the different elements that already have been demonstrated in LNOI, we will highlight the advantages this platform has for quantum photonics.

2.1. Fundamental Advantages of the LNOI Platform

Before discussing specific elements for quantum photonics, we are looking at the general properties and advantages of the LNOI platform that makes it attractive for integrated optics in general and quantum photonics in particular. The material lithium niobate is well-established in optics for its advantageous properties. These are mainly the large transparency range, which stretches from a wavelength of 350 to 4.5 μm , and its second-order nonlinearity, which enables nonlinear frequency conversion and fast modulation of light using the electro-optic effect. This enables to generate and control light from the UV^[17,18] to the mid-IR spectral range.^[19,20] In quantum optics, this particularly opens a path to specific sensing schemes that rely on strongly degenerate photon pairs.^[21,22] The advantages of lithium niobate were also recognized in integrated optics and low-loss waveguide technologies were developed already decades ago^[23–25] and already have been used for integrated quantum photonics.^[8,26,27] However, the used waveguide technologies rely on the indiffusion of titanium or proton exchange, which results in a small change of the refractive index that leads to weak guiding and comparably large waveguide cross-sections, limiting the complexity of integrated circuits to a few different functional elements.^[28–31]

2.1.1. LNOI Allows Nanostructuring

To use integrated quantum photonics for the realization of applicable quantum protocols on a chip, hundreds or thousands of individual functional elements will be necessary, especially for photonic quantum computing.^[4,32,33] This necessitates a waveguide technology that allows for small waveguides that

compress light transversally into tiny areas such that many waveguides can be densely integrated without unwanted crosstalk. Furthermore, a variable and precise control of the modal properties in these waveguides is needed, that enables to tailor the used photonic quantum states to the needs of the targeted applications. These requirements can be met by waveguides with a large refractive-index difference between core and cladding created by nanostructuring technologies, that is, by selectively removing the LN material.

However, nanostructuring of LN is challenging, as this crystalline material is very hard and chemically inert. In particular, realizing a large index difference to the substrate while keeping the crystallinity of the waveguide material unchanged is complicated, although possible with ion-beam enhanced etching techniques.^[34–37]

This situation was changed notably with the development of crystal ion slicing,^[38,39] which enabled the creation of thin slabs of crystalline lithium niobate^[40] bonded to another dielectric substrate. Based on this technology, which was commercialized in the last years, different approaches for the creation of waveguides have been explored, including proton exchange,^[41] dicing,^[42–44] ion-beam enhanced etching,^[45] focused-ion-beam milling,^[46] and femtosecond-laser micromachining with subsequent polishing.^[47,48]

However, the most promising structuring approach is based on lithography and dry etching.^[49–52] This approach is sketched in **Figure 1a** and is very similar to the methods used in silicon photonics and other established technology chains for integrated optics. It enables large-scale fabrication of integrated optical circuits^[32,33] with arbitrary lateral geometries, which has already been demonstrated in LNOI.^[53] Based on this technology, many functional elements that are needed for integrated quantum photonics have been demonstrated, albeit in mostly different contexts, like waveguides (see example in **Figure 1b**),^[54] couplers, filters, and resonators (**Figure 1c**).^[55] Most importantly, these waveguide structures feature exceptionally low losses as small as 3 dB m^{-1} in the near-infrared (NIR),^[56] comparable to silicon photonics. However, compared to silicon LNOI can provide such small losses over a much broader spectral range and losses of 6 dB m^{-1} were demonstrated in the visible spectral range.^[55] Low losses are one of the most crucial requirements for quantum photonics, as particularly entanglement is very sensitive to loss-induced decoherence.

Due to the relatively large refractive index difference between waveguide structures etched in LNOI and the surrounding cladding media, not only ridge-waveguide-based structures but also more complex nanophotonic structures have been realized in this platform, ranging from photonic crystals^[46,57–61] (**Figure 1d**) to resonant metasurfaces^[62–65] (**Figure 1e**). Such structures promise a large degree of freedom in the control of the spatial and spectral properties of the modes in quantum-photonics devices, which is very useful to tailor the properties of photonic quantum states.^[66,67]

2.1.2. LNOI has $\chi^{(2)}$ Nonlinearity

One of the main advantages of LN in comparison to many other established material systems for integrated optics in general

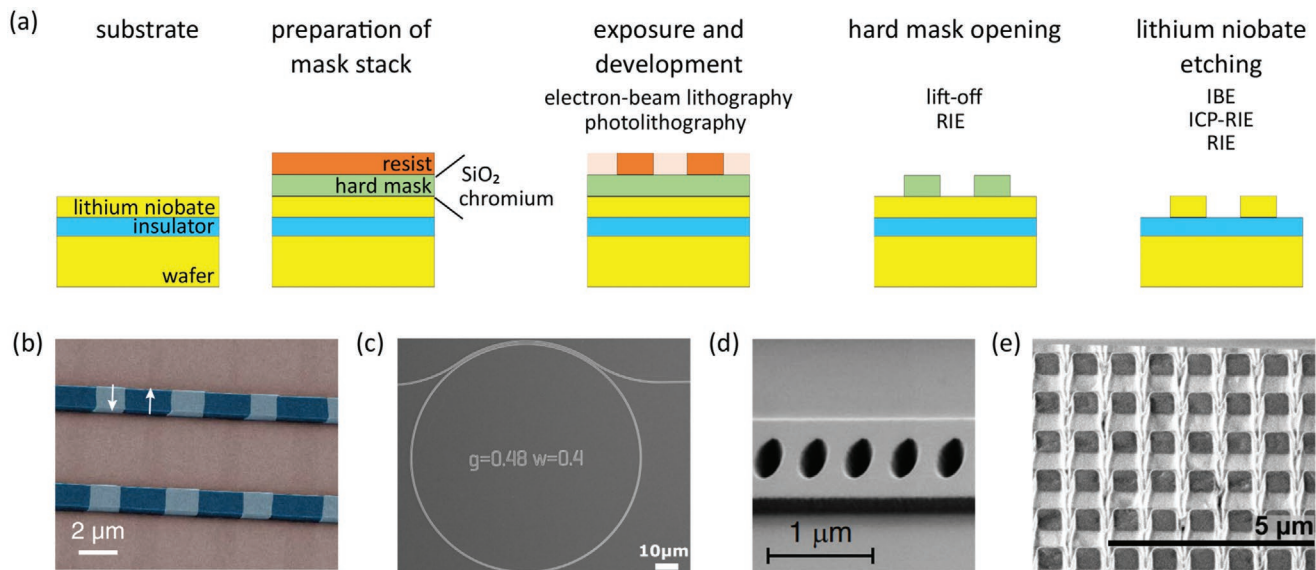


Figure 1. a) Scheme of typical processing steps for nanostructuring LNOI with some characteristic examples for the used processes and materials. Starting from the substrate material, first a mask stack is realized, where typical materials for the hard mask needed for the central etching step are chromium or SiO₂. The top resist layer is then typically exposed by electron-beam or photo-lithography and processed such, that in a next step the hard mask can be opened using a lift-off process or reactive ion etching (RIE). Finally, the lithium niobate layer can be structured using ion-beam etching (IBE), inductively-coupled plasma RIE (ICP-RIE), or RIE. b–e) Example structures made with processes similar to (a), in particular b) waveguides, where the different shadings indicate periodic poling,^[54] c) ring resonator,^[55] d) detail of photonic-crystal cavity,^[57] and e) metasurface. (b) Reproduced with permission.^[54] Copyright 2018, The Optical Society. (c) Reproduced with permission.^[55] Copyright 2019, The Optical Society. (d) Reproduced under the terms of a Creative Commons Attribution 4.0 International License.^[57] Copyright 2020, The Author(s), published by Springer Nature.

and integrated quantum photonics, like silicon or silicon nitride in particular, is its second-order nonlinearity, described by the second-order nonlinear tensor $\chi^{(2)}$. Rooted in the absence of centro-symmetry in the crystal lattice of LN, the $\chi^{(2)}$ nonlinearity enables nonlinear frequency conversion via parametric three-wave mixing processes across a wide spectral range. This is particularly relevant for the generation of quantum light, as it allows for spontaneous parametric down conversion, where one pump photon is split into a pair of signal and idler photons sharing a common quantum state.

In LN, the $\chi^{(2)}$ nonlinearity can be conveniently controlled by local inversion of the LN crystal lattice, for example, by electric-field poling.^[68] This process switches the sign of the elements of the $\chi^{(2)}$ nonlinear tensor while leaving the linear properties of LN unchanged. If LN is poled in a periodic pattern along the propagation direction of waves undergoing frequency conversion, an additional wavevector is introduced, which can be used to offset the phase mismatch between the interacting waves by quasi-phase matching. Quasi-phase matching enables to achieve phase matching, and thus efficient nonlinear interactions, independent of the linear properties of the optical system. This is particularly important for waveguides, where now the same waveguide geometry can be used with different poling periods to enable efficient frequency conversion between arbitrary spectral ranges.

Periodic poling has been an established technology for bulk and integrated optics in LN since many years.^[68] However, due to the specific properties of LNOI, which made the use of existing poling approaches challenging, new strategies had to be developed. Whereas typically the electrodes to apply the high voltage needed for domain inversion are applied at the top and

bottom sides of z-cut LN, in LNOI x-cut films are poled with both electrodes located at the top of the substrate.^[52,69] Since the electrodes in this technique can be placed quite close to each other, small poling periods in the micrometer range and below can be realized with high quality.^[70–72] This can be used to overcome even larger phase mismatches, which can occur in frequency conversion schemes where the participating waves travel in different directions.^[73] Thus, due to electric-field poling and quasi-phase matching, LNOI enables phase-matching geometries for classical and quantum frequency conversion that go far beyond what is possible in other photonic integrated platforms. This phase-matching technique is compatible to the nanostructuring process described above.

The phase-matching techniques described above together with the strong mode confinement in LNOI waveguides and their small losses have led to a number of demonstrations of very efficient classical frequency conversion. SHG with high conversion efficiency was shown in waveguides^[54,74,75] and ring resonators.^[76] Furthermore, sum-frequency generation was shown in resonators^[77] and waveguides.^[78] As these parametric three-wave mixing effects are governed by the same rules as spontaneous parametric down conversion for the generation of photon pairs, these results bode very well for their efficient generation, which will be discussed later. Besides these nonlinear effects directly relevant for quantum photonics, other observed nonlinear effects include supercontinuum generation,^[79] micro-comb generation,^[80–83] and the conversion of mechanic and acoustic vibrations to the optical domain.^[84,85]

In addition to these nonlinear frequency conversion processes, the second-order nonlinearity in LN also enables to effectively change the linear properties of the material via an

Table 1. Comparison between different platforms considered for realization of large-scale integrated quantum photonics.

Parameter	LNOI	Silicon ^[90]	Silicon nitride ^[91]	Gallium arsenide ^[92]
Transparency window	Visible–infrared	infrared > 1000 nm	Visible–infrared	Infrared > 900 nm
Propagation loss in etched single-mode waveguides	Low linear loss no nonlinear loss	Low linear loss high nonlinear loss (two-photon absorption)	Low linear loss nonlinear loss (two-photon absorption)	Low linear loss no nonlinear loss
Modulation mechanism	Electro-optic effect	Thermal (slow) free-carrier injection (induces losses)	Electro-static devices MHz bandwidth	Electro-optic effect
Mechanism for quantum-state generation	SPDC	SFWM	SFWM	SPDC, quantum dots (single photons)

externally applied voltage through the electro-optic effect. This effect has been used to implement modulators working at CMOS-compatible voltages,^[86] and at modulation bandwidths in the range of hundreds of GHz.^[87–89]

The ability to create high-quality waveguides with tight confinement allows for dense waveguide networks with minimal dissipation. Due to the electro-optic effect, these networks can be reconfigured, thus enabling, for example, the implementation of tunable quantum gates. Finally, the second-order nonlinearity straightforwardly allows for the generation of many different photonic quantum states, which in turn can be tailored using the degrees of freedom enabled by tightly confining waveguides. These fundamental properties and advantages make LNOI an attractive platform for integrated quantum photonics, which is on par with other, more established platforms^[90–92] as can be seen in the direct comparison in **Table 1**. In the following, we will overview more specifically the individual elements needed to implement versatile quantum circuits in integrated-optical platforms and the status of their realization in LNOI. We will first discuss sources of photonic quantum states, then functional elements for their manipulation and storage, and finally detection and interfacing to other systems for quantum applications.

2.2. Sources for Photonic Quantum States

The most prominent way for quantum light generation in materials with second-order nonlinearity is by spontaneous parametric down-conversion (SPDC), where a short-wavelength pump photon is spontaneously split into a pair of signal and idler photons of longer wavelengths.^[93] The three-photon process has to conserve energy, thus the frequencies of pump (p), signal (s), and idler (i) have to obey $\omega_p = \omega_s + \omega_i$. Furthermore, efficient nonlinear interaction is facilitated by vanishing phase mismatch, such that the propagation constants of the interacting modes fulfill $k_s + k_i = k_p$.

Compared to photon-pair generation by spontaneous four-wave mixing (SFWM), which is based on third-order nonlinearity and prominently used in integrated quantum optics based on silicon and silicon nitride,^[94–97] SPDC can typically make use of a much larger nonlinear coefficient, thus enabling efficient photon-pair generation with lower pump power and/or shorter waveguides. On the other hand, the typically large difference in the wavelengths of the interacting waves in SPDC leads to larger phase mismatches, which in LNOI have to be mitigated using quasi-phase matching. Furthermore, the different

wavelengths have to be taken into account when designing quantum waveguide platforms making use of SPDC.

SPDC and the emission of photon pairs in LNOI have been first demonstrated in a micro-disk resonator coupled by a fiber taper.^[98,99] Furthermore, photon-pair generation was recently demonstrated in a fully integrated ring resonator,^[100] shown in **Figure 2a**, with photon-pair rates up to 36 MHz using just 13 μW pump power and coincidence-to-accidental ratios of up to 15,000. In periodically poled waveguides, pair generation was demonstrated^[101–105] with photon-pair rates up to 11 MHz for pump powers of 250 μW and maximal coincidence-to-accidental ratios of close to 70,000^[101] as shown in **Figure 2b**. Due to the high efficiency, appreciable photon-pair rates can be generated in very short waveguides of only 300 μm length,^[103] and over a broad spectral range.^[102,103,106]

These first demonstrations are very encouraging for a use of such sources in integrated quantum photonics, as the reported count rates are already comparable or even better than that of optimized silicon-photonics sources,^[107] even without employing techniques like the use of slow light^[108] for enhancement of the generation efficiency. In LNOI, the degrees of freedom offered by nanostructuring can be fully exploited for controlling the properties of the generated quantum state, for example, its spatial^[66,73] and spectral composition.^[67,109]

Whereas photon pairs are the basis for quantum applications in quantum cryptography, imaging,^[110] and some implementations of photonic quantum computation algorithms,^[111] sources of pure single photons are needed for universal quantum computing.^[112] Pure single photons can be generated with photon-pair sources using heralding,^[113–115] where only one of the photons of a pair is used as a quantum resource, whereas the other heralds the presence of this resource. To achieve this, the two photons of a pair have to be in a spectrally factorizable state, which can be realized by dispersion engineering of LNOI waveguides.^[109] One of the drawbacks of such heralded single-photon sources and SPDC sources in general is their probabilistic operation, where there is a low probability of generating a pair per input pump pulse. To overcome this limitation, several such probabilistic sources can be combined by multiplexing,^[116] thus increasing the likelihood of generating a single photon in a given time frame. We will discuss in depth the potential of the LNOI platform for the implementation of such multiplexed sources in the second part of this report.

On the other hand, pure single photons can also be deterministically created using atomic emitters or quantum dots.^[117] The material LN naturally does not provide suitable color centers or similar atom-like defects suitable as single-photon

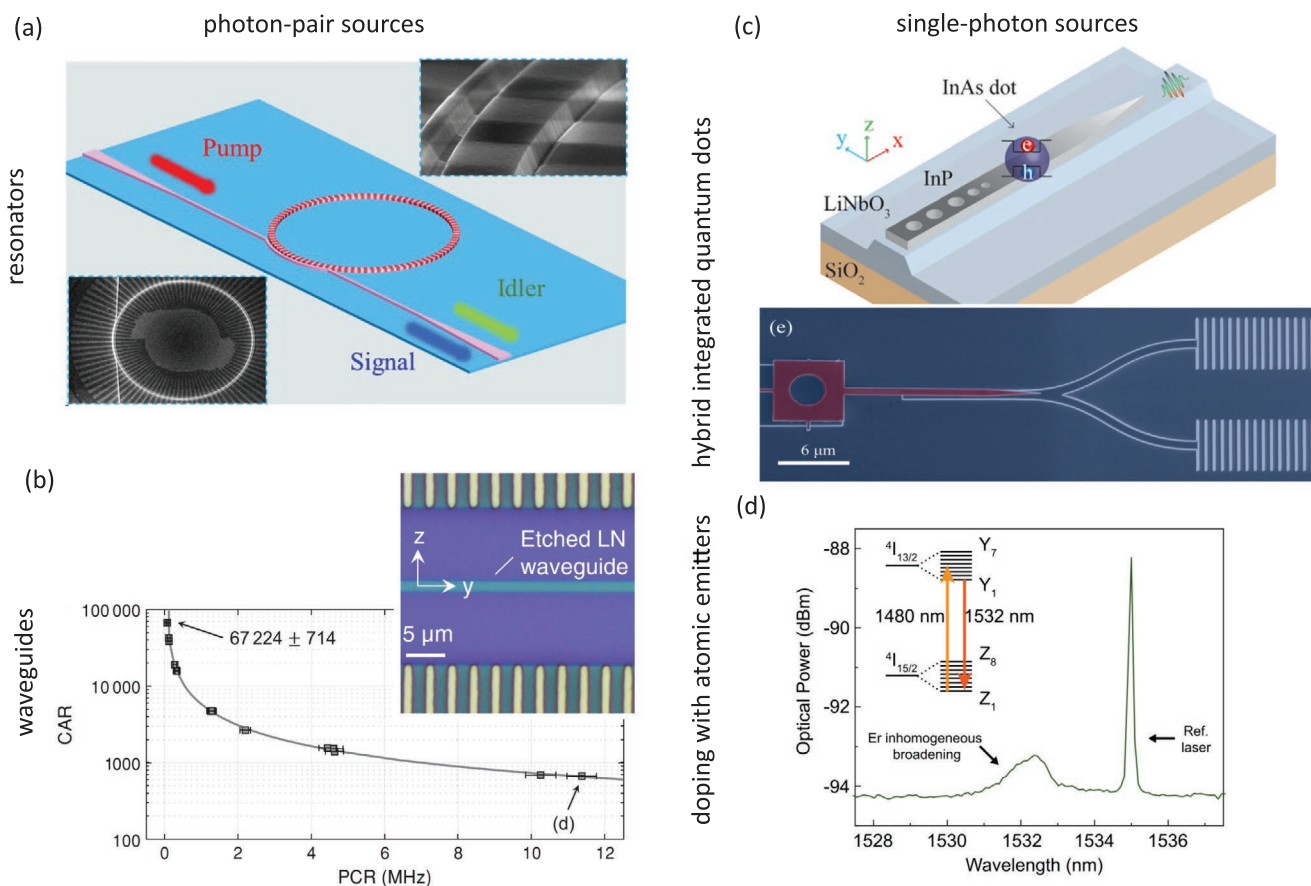


Figure 2. Overview of different quantum-state sources. a) Sketch and SEM images of LNOI ring resonator for photon-pair generation.^[100] b) Microscope image of waveguide for photon-pair generation and measured dependence of coincidence-to-accidental ratio (CAR) on pair coincidence rate (PCR).^[101] c) Sketch and SEM image of hybrid structure incorporating an InAs quantum dot in a LNOI waveguide.^[127] d) Emission spectrum of erbium ions implanted in LNOI resonator, demonstrating the possibility to also incorporate atomic emitters.^[119] (a) Reproduced with permission.^[100] Copyright 2020, American Physical Society. (b) Reproduced under the terms of a Creative Commons Attribution 4.0 International License.^[101] Copyright 2020, The Author(s), published by the American Physical Society. (c) Reproduced with permission.^[127] Copyright, AIP Publishing. (d) Reproduced with permission.^[119] Copyright 2020, AIP Publishing.

sources. However, such centers could be created by selective doping of the LN host material. Doping of LNOI has been demonstrated with Tm,^[118] Er,^[119–124] and Yb ions,^[125,126] which were used to demonstrate photoluminescence, amplification, and lasing. Semiconductor quantum dots can be added to the LNOI platform by hybridization, where a semiconductor structure containing a quantum dot is coupled to a waveguide in LNOI by specifically designed tapers.^[127]

Finally, some quantum-photonics applications are not based on number states of light like the single photons and photon pairs discussed above, but rather use squeezed light as an input.^[128] Although squeezed-light generation was not yet demonstrated in LNOI, it was shown in LN waveguides^[129–131] and it is very likely that similar results are possible also in LNOI, especially that ultralow-threshold optical parametric oscillation using a quasi-phase matched microring resonator have already been demonstrated on the LNOI platform.^[132]

These different experimental demonstrations in LNOI show that this platform is promising for the implementation of all types of quantum-state sources.

2.3. Manipulation and Storage of Quantum States

After discussing approaches for the generation of photonic quantum states on the LNOI platform, we will now examine the potential to also implement functional elements to control such quantum states. Control in this respect means the ability to influence the degrees of freedom of the photons contained in a quantum state, for example, their spatial distribution, polarization, spectrum, and also temporal distribution. We will first discuss passive, that is, fixed elements, then tunable active control elements before finally discussing separately elements to control time, that is, quantum memories.

2.3.1. Passive Manipulation

The purpose of functional elements for passive manipulation is to connect different optical modes and thus to transfer or distribute photons between them. In the spatial domain, this is typically achieved using directional couplers, y-splitters, or

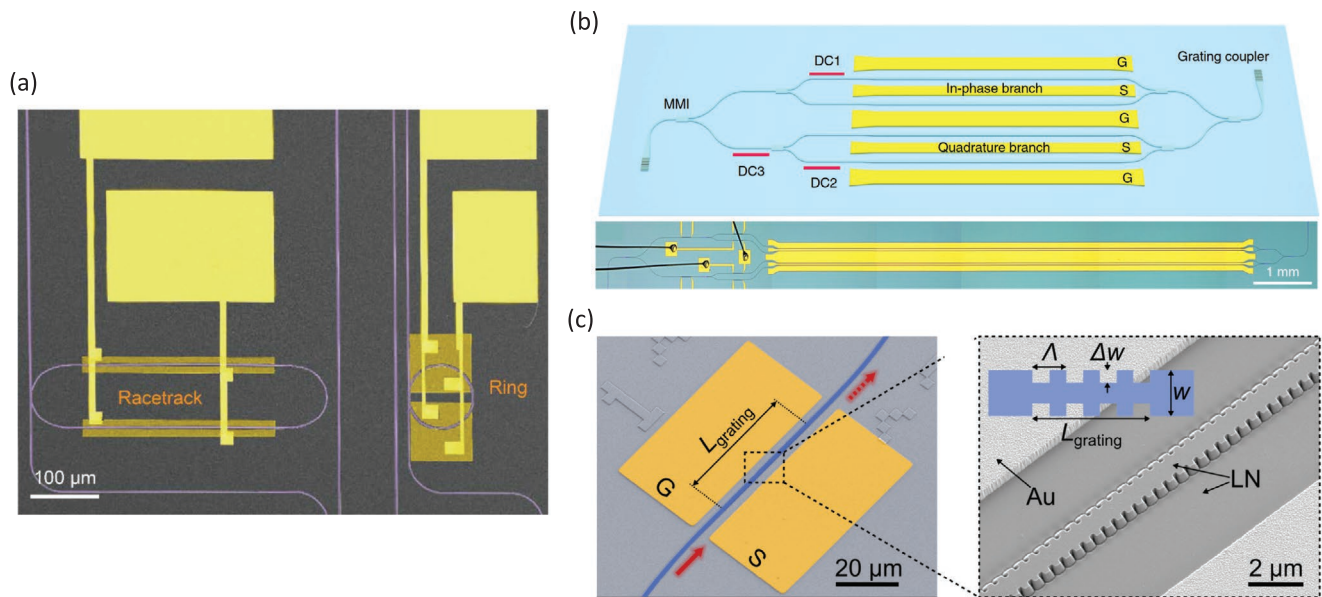


Figure 3. Modulators implemented in LNOI. a) Racetrack and ring resonators,^[149] b) scheme and microscope image of modulator for amplitude and phase based on interferometer quadrature,^[147] and c) modulator based on tunable Bragg grating.^[152] (a) Reproduced with permission.^[149] Copyright 2018, The Optical Society. (b) Reproduced under the terms of a Creative Commons Attribution 4.0 International License.^[147] Copyright 2020, The Author(s), published by Springer Nature. (c) Reproduced under the terms of a Creative Commons Attribution 4.0 International License.^[152] Copyright 2020, The Author(s), published by IEEE.

multi-mode interference splitters which are routinely fabricated in LNOI.^[55,133–135]

LN is a birefringent material. In LNOI waveguides, typically the extraordinary crystal axis is oriented transverse to the propagation direction, which together with the typical waveguide cross-sections leads to a strong modal birefringence. This enables to use the polarization degree of freedom for quantum-optical functionalities. Spatial routing of photons based on their polarization was demonstrated using a specifically designed directional coupler,^[136] which can operate over a large spectral range using an adapted design.^[137] Finally, waveguides in LNOI can also be designed to show no modal birefringence,^[138] thus leading to degenerate propagation constants for both polarization modes.

For control of the spectrum, demonstrated wavelength filters include Bragg reflectors created by periodically indenting the waveguide surface.^[139–141] To achieve higher extinction and narrower linewidth, which in integrated quantum photonics is usually needed to filter out the strong classical pump beam, resonators^[142] or interferometric filters^[143] are usually applied. In LNOI, high-quality resonators and interferometers suitable for this task have been demonstrated, especially also in the near-visible spectrum where the pump beams would be situated for photon-pair generation in the telecom frequency range.^[55] However, these configurations have not yet been used specifically for frequency filtering in quantum applications.

Aside from the mentioned linear passive optical elements, a highly desirable functionality is to have passive elements that can exhibit substantial optical nonlinearity at the single-photon level. The LNOI platform has shown promise toward reaching this goal, where leveraging the high nonlinearity and fabrication quality on LNOI, single-photon anharmonicity close to 1% has

been reached using a microring resonator.^[144] It was also theoretically proposed^[144] that future improvements could increase this number and eventually allow for the photon blockade effect, which would be a path toward emitter-free, deterministic, and all-optical quantum operations at room temperature.

2.3.2. Active Manipulation

To implement universal quantum functionalities, like gates for quantum computations, the needed integrated optical elements shall be dynamically tunable. Besides fundamentally investigated all-optical switching schemes,^[145] the most relevant tuning mechanism in LN is the electro-optic effect, which allows to change the refractive index of the materials upon application of an electric voltage. An alternative is thermo-optic tuning, which is often used in silicon photonics,^[33] and has been implemented in LNOI as well.^[146,147] However, thermo-optic modulators are limited in their speed by the heat transfer in LN. In contrast, electro-optic modulators in LNOI waveguides can be operated at low voltages and high speeds due to the small waveguide dimensions and high field confinement compared to conventional indiffused waveguides. The potential of LNOI for the realization of modulators was recognized early.^[49] Modulator concepts can be based on resonators, where the applied voltage shifts the resonance frequency, such that the transmission of an adjacent bus waveguide can be modulated,^[148,149] on interferometers, where the phase shift induced by a phase-only modulator in one of the arms^[150,151] leads to amplitude modulation at the interferometer output,^[86,149] or on Bragg reflectors, where the applied voltage shifts the reflection band^[152] or cavity resonances.^[153] Examples for these realization concepts are shown

in **Figure 3a–c**, respectively. Based on interferometers, also universal modulators controlling amplitude and phase have been demonstrated.^[147] Modulators in LNOI show very promising features, such as small modulation voltages in the CMOS-compatible range suitable for direct interfacing with standard electronics,^[86,154,155] modulation speeds above 100 GHz and up to 400 GHz,^[87–89] extinction ratios of up to 53 dB using a cascaded design,^[156] and small form factors.^[57,89] Although most of these demonstrations focused on the realization of modulators for the amplitude of transmitted light, integrated quantum photonics is built on phase shifters, which are the heart of interferometer-based amplitude modulators, and switches, which can be realized by utilizing both output waveguides of a tunable Mach–Zehnder interferometer.^[157–159] These functionalities enable the realization of tunable photonic quantum gates for the spatial modes, which is the basis for integrated quantum optics using the path degree of freedom.

To implement quantum gates that operate on the spectral degrees of freedom, it is necessary to not only filter the spectrum, but transfer energy from one spectral mode to another. This is typically achieved by nonlinear frequency conversion, for example, by sum–frequency conversion, which in the classical realm has been demonstrated in LNOI.^[60,77,160] For quantum applications, high conversion efficiencies are needed to do this at the single-photon level, which should ideally be done with 100% efficiencies and no added noise. Recently, such quantum frequency conversions^[161] from telecom to near visible has been demonstrated with a periodically poled LNOI waveguide with an internal efficiency close to 50% and a noise level of 10^{-4} photons per time–frequency mode.^[162] Using nonlinear frequency conversion allows to bridge large differences in the source and target frequencies, however, using fast electro-optic modulation, optical signals can be shifted sufficiently to bridge, for example, the frequency difference between ITU grid channels.^[163] Using the electro-optic effect on the LNOI platform with two coupled microring resonators, GHz-range frequency shifts with near-unity efficiencies have been demonstrated,^[164] where the conversion efficiency is also tunable, further allowing for the implementation of frequency beam splitters. Frequency shifts in the electro-optically induced gratings also enable the realization of periodic reflectors acting as dynamically switchable spectral filters.^[165] Thus, the possibilities for controlling the spectrum of quantum signals in LNOI may be unrivalled by any other integrated optical platform.

Finally, also the polarization can be dynamically controlled, where coupling between the two polarization states in a waveguide can be implemented using periodically poled waveguides, which upon the application of a static electric field act like a coupling grating.^[78,165] This concept already has been applied to polarization control of single photons in an LNOI waveguide.^[166]

2.3.3. Storage of Quantum States

The delay or storage of photonic quantum states is a crucial capability in complex quantum circuits and networks, either to offset the probabilistic nature of spontaneous nonlinear photon sources, to synchronize different functionalities on one optical

chip, or to implement quantum communication. The simplest way of implementing such storage is by employing long waveguides, in which the propagation time equates the storage time. Due to the small losses in LNOI, such long waveguides can be implemented and have been demonstrated with lengths exceeding 1 m, which equates to delay times in the order of 8 ns, on optical chips with dimensions in the range of tens of mm as shown in **Figure 4a**.^[157] Such delays can be dynamically controlled with high speed using electro-optical switches^[157] or electro-optically induced gratings, that reflect photons at different positions in the waveguide.^[136]

A much more compact scheme for photon storage has also been realized on the LNOI platform based on two coupled microring resonators and application of the electro-optic effect.^[167] The coupled system of resonators has a dark and bright mode, where an incoming optical pulse from a coupled ridge waveguide can couple to the bright mode. Then through the application of a microwave pulse faster than the lifetime of the bright mode, which is allowed by the fast electro-optic effect, the optical pulse will be transferred into the dark mode and trapped there. After the desired time delay, a second microwave pulse will transfer the optical pulse back to the bright mode to be released. The storage time in this scheme is only limited by the lifetime of the dark mode, which is around 2 ns here. The authors in ref. [167] predict that if the fabrication technology in LNOI can be pushed to its limit of material absorption, the storage time of this tunable device could reach hundreds of nanoseconds.

Quantum memories are typically implemented using atomic systems, which can absorb the signal photons and release them after a defined storage time. This has been demonstrated in conventional waveguides in LN using doping with Tm ions.^[170] Doping of LNOI with such ions has been successfully demonstrated,^[120] where the measured emission spectra shown in **Figure 4** are similar to the ones measured in other material system. Hence, the implementation of quantum memories also in the LNOI platform appears feasible.

2.4. Interfacing and Hybridization

Although many functionalities can be implemented directly on photonic integrated chips based on LNOI, further means to interface such chips to other devices and systems are needed to realize additional functionalities. This includes the detection of photons for connection to electronic circuitry, the highly efficient coupling to fibers for integration in optical networks, and the hybridization with other material platforms that can provide specific functions.^[7]

2.4.1. Detection

The detection of photonic quantum states is the key to measure the result of any photonic quantum operation. Although many demonstrations have been conducted using separate detectors, which were connected to the integrated chips by optical fibers, chip-integrated detectors offer to minimize the coupling losses inherent in these connections. In

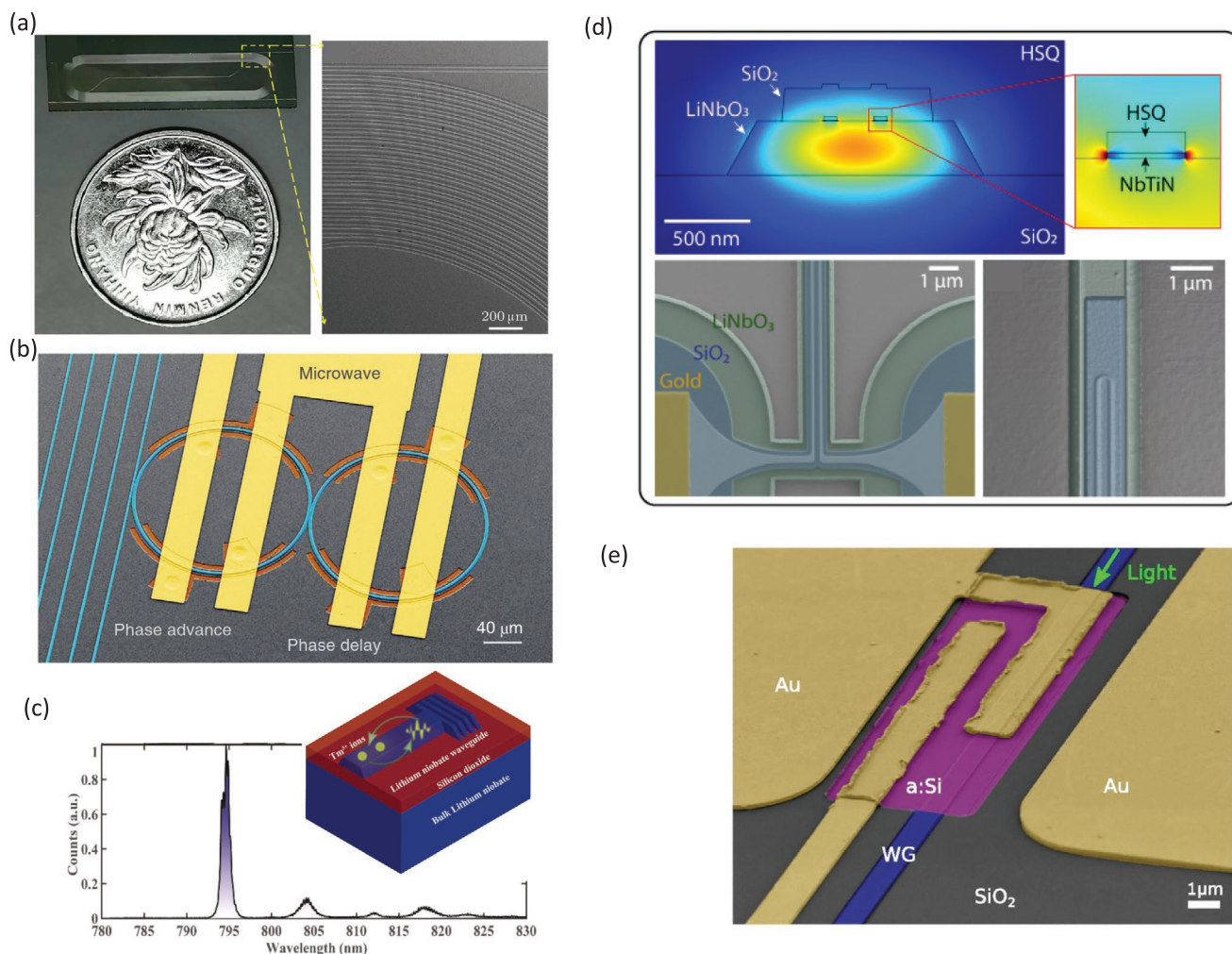


Figure 4. Functional elements for quantum photonics on LNOI chips. a) Meter-scale delay line^[157] and b) photonic molecule for storage of photons.^[167] c) Demonstration of Thulium doping showing a scheme of the implemented device and the measured emission spectrum,^[120] which can be developed toward a quantum memory in LNOI. d) Cross-section and false-color SEM images of LNOI waveguide with integrated superconducting nanowire single-photon detector.^[168] e) False-color SEM image of silicon photodetector integrated with LNOI waveguide.^[169] (a) Reproduced with permission.^[157] Copyright 2020, Chinese Physics Letters. (b) Reproduced with permission.^[167] Copyright 2018, The Author(s), under exclusive licence to Springer Nature Limited. (c) Reproduced with permission.^[120] Copyright 2019, American Chemical Society. (d) Reproduced with permission.^[168] Copyright 2021, The Author(s). (e) Reproduced with permission.^[169] Copyright 2019, AIP Publishing.

recent years, superconducting nanowire single-photon detectors (SNSPDs) became the state of the art for efficient and broadband single-photon detection, especially in the telecom wavelength range.^[171] SNSPDs have also been integrated onto on-chip optical waveguides in different material platforms,^[172] with recent implementations on LNOI waveguides as well.^[168,173,174] ref. [173] reached a detection efficiency of 46% at 1560 nm, with an SNSPD of only 250 μm length integrated on an LNOI ridge waveguide of 125 μm length. A low dark-count rate of 13 Hz and a timing jitter of 32 ps was achieved in this implementation. Moreover, ref. [168] have implemented two SNSPDs and an electro-optic switch integrated on the same LNOI chip and demonstrated their successful combined operation at cryogenic temperatures, which is an important step toward a full on-chip implementation of fast-reconfigurable optical quantum circuits on the LNOI platform.

Alternatively, photon detection can be also realized using semiconductor detectors, as have been also integrated on LNOI.^[169] Although the sensitivity of these devices is not yet high enough to detect single photons, these results underline the potential to also realize avalanche photodiodes or fast detectors suitable for the characterization of squeezing.

2.4.2. Interfacing to Other Platforms

The most important interface to other photonic platforms is the coupling to optical fibers, which is needed to transfer photons into networks, to separated optical chips,^[175,176] to external detectors, or to external fiber delay lines. Achieving a highly efficient coupling between LNOI waveguides and optical fibers is not trivial, as these two platforms have

strongly differing mode-field diameters. One approach is by using grating couplers, to which optical fibers can be attached from above the optical chip. Such couplers have been demonstrated in several works^[139,177–180] with coupling efficiencies up to 72%. Grating couplers use resonances for efficient coupling, thus limiting the spectral range in which they work. An alternative approach is based mode converters, which change the geometry of the waveguide to adapt the mode at the edge of a photonic chip to the modes of a butt-coupled fiber. Such structures, which are conceptually similar to inverse tapers known from silicon photonics,^[181] have been demonstrated in LNOI as well^[182–186] with measured coupling efficiencies close to 90% to tapered or lensed optical fibers. Although these results are encouraging, they still have to be improved to not be a hindrance in the implementation of quantum devices, especially if several photons should be transferred from or to a photonic chip.

Furthermore, LNOI functional elements have been successfully integrated with other photonic platforms that are used for integrated quantum photonics, for example, silicon^[87,187,188] and silicon nitride.^[189–191] Finally, LNOI waveguides can be also interfaced with superconducting quantum circuits, as optical-to-microwave transducers have been recently demonstrated.^[192–194] The LNOI platform can thus be connected to a multitude of different systems used in quantum technologies.

This overview of realized functional elements for quantum photonics shows, that most of the needed elements already have been realized in LNOI, although reports on more complex integrated quantum experiments are still missing. However, with the demonstrated wealth of structures, many of the experiments shown in other platforms can in principle be implemented.

3. Implementation of a Complex Quantum Chip on the LNOI Platform

In this section, we evaluate the feasibility of the on-chip realization of complex quantum systems using the LNOI platform. We approach this by investigating a particular example for which we quantify the performance and discuss the areas that the current technology needs to be improved. Our representative example of investigation is the on-demand source of indistinguishable single photons, the realization of which at the moment is arguably the biggest challenge and a bottleneck toward the large-scale implementation of optical quantum computation and simulation protocols.^[2,3] In this regard, single-photon sources are the fundamental resource for generation of cluster states to perform all-optical quantum computations.^[195] They can also be used for the generation of three photon Greenberger–Horne–Zeilinger states,^[196] which itself is a fundamental resource for certain approaches for linear optical quantum computation,^[197,198] multiparty quantum key agreement,^[199] quantum secure direct communication,^[200] and all-optical quantum repeaters.^[201] Single-photon sources are also the fundamental resource for the implementation of Boson sampling,^[2] which is thought of as a path toward reaching non-universal quantum supremacy in computation in the near future. In all such applications, few to many single photon

sources are needed, which ideally need to be indistinguishable from one another and produce single photons on demand.

3.1. Spatial Multiplexing for On-Demand Single-Photon Generation

One promising approach for realizing such sources is through multiplexing SPDC-based heralded single-photon sources (HSPSs). As explained earlier, HSPSs are probabilistic and multiplexing is used to approach an on-demand operation.^[118] However, HSPS multiplexing schemes are resource-hungry, and approaching the ideal performance often requires more and more components, including SPDC sources, single-photon detectors, delay lines, and fast switches, along with fast electronics to synchronize the operations. Hence, integration of such components in a miniaturized form is needed to parallelize as many HSPSs as necessary for achieving the desired photon statistics. To this date however, there has not yet been a fully integrated implementation of such a system, with all the components on the same chip, which in turn hindered reaching a performance that can live up to the requirements for large-scale quantum computing and simulation protocols.

We believe that the unique advantages of the nanostructured LNOI platform could open up a way toward a fully integrated multiplexed source, as it allows for efficient and engineered pair generation along with low-loss and fast switching. Both are central requirements for any multiplexing scheme. To explain this vision and benchmark the capabilities of the LNOI platform for this application, we focus on the spatial multiplexing scheme,^[202] which we believe all the optical components for its on-chip realization in principle exists on the LNOI platform. There are also other types of multiplexing schemes for on-demand single photon production, such as temporal and spectral multiplexing,^[118] which we do not discuss here. Nonetheless, their on-chip implementation relies on the same fundamental components that will be discussed here.

In spatial multiplexing, many HSPSs are used in parallel, as shown schematically in **Figure 5**. The schematic here also specifically depicts our vision for a full on-chip implementation of spatial multiplexing, based on the components available on the LNOI platform, where the steps of the operation and the depictions of the components are based on our discussions to follow. The HSPSs must all be identical to each other and each produce factorizable photon pairs, such that detection of one photon for heralding does not disturb the quantum state of the other photon at the output. To avoid multiple-pair generation, the generation probability of each HSPS has to be kept sufficiently low. Multiplexing is used to increase the total generation probability. One photon from each HSPS goes to a single-photon detector and the other photon to a routing network of switches, which is controlled electrically by the collective response of the detectors. The response from all the detectors will be analyzed to identify which HSPSs have produced a pair, then the single photon from only one of the corresponding HSPSs will be routed to the output. In this way, the probability P of having an output is increased, while maintaining a high fidelity F , where F indicates how much the output overlaps with a pure single-photon state, with $F = 1$ being the ideal case.

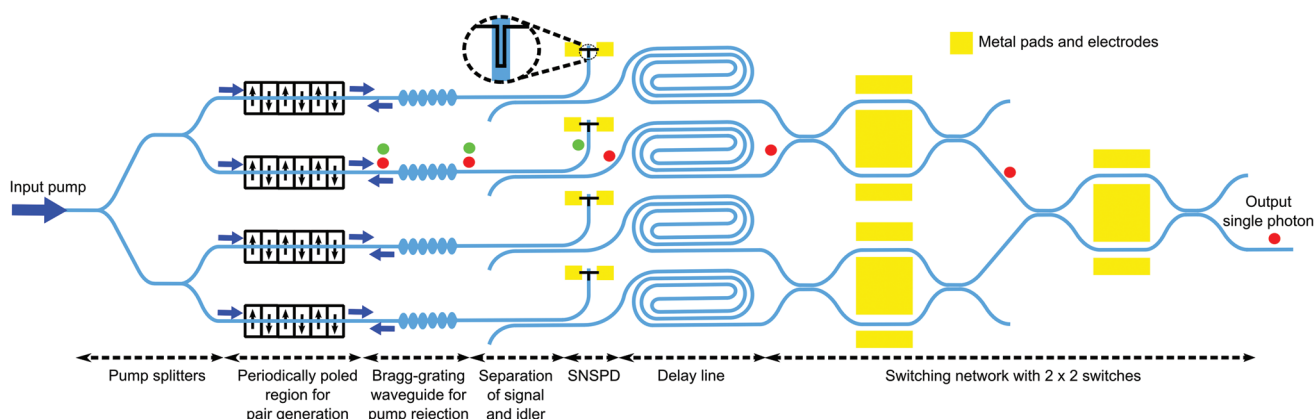


Figure 5. The envisioned fully on-chip implementation of a spatially multiplexed single-photon source on the LNOI platform, where only 4 sources are shown in the schematic for a clearer view. The metal pads for the SNSPDs and the metal electrodes for the switches can be connected to a nearby electrical chip by flip-chip bonding.

To increase P and F simultaneously, an increasing number of sources must be used, due to the fundamental trade-off between fidelity and generation probability in the SPDC process underlying each HSPS. For example, assuming that we have HSPSs with perfectly factorizable pairs, ideal detectors, and no loss, then $F = P = 0.99$ requires 458 HSPSs. This number is calculated based on the existing formulations for estimating the performance of a multiplexed single-photon source,^[118,203] assuming that threshold (non-number-resolving) detectors are used. If photon-number-resolving detectors are used, that can distinguish between one and more than one photon, then HSPSs can be operated at a higher gain and only 17 sources are needed to reach $P = 0.99$ with a fidelity of $F = 1$, as multiple-pair events can be discarded.^[118,203] If the detection efficiency is lower, then more HSPSs are needed.^[118] With number-resolving detectors, a lower detection efficiency also affects the fidelity, as identifying multiple-pair events is less reliable. Hence, the source gain has to be lowered to reach the needed fidelity, which increases the needed number of sources to reach the same output probability.^[204] If the sources are not fully factorizable, there would be a limit on the fidelity that cannot be offset by using more sources. If the path of single photons from the source toward the output channel is lossy, then the output probability will be lowered, which again cannot be offset by having more sources.^[204] It is clear that the only practical way of realizing such a system is through a fully integrated approach, with a careful balance of miniaturization, loss, and tolerancing.

3.2. Performance Evaluation of Required Components for On-Chip Spatial Multiplexing

To realize such a system fully on chip we need i) SPDC-based photon-pair sources that can produce factorizable pairs, ii) spectral filters and waveguide couplers to separate the photon pairs from each other and from the pump, iii) fast on-chip single photon detectors, iv) fast optical switches with CMOS compatible driving voltages, v) fast on-chip electronics to drive the switches, and vi) delay lines to compensate for the latency in the electronic response. In the following, we discuss the

currently achievable performance of these individual components on the LNOI platform with regards to the multiplexing application and quantify the total performance of a potential multiplexed source, where some assumptions are made as to what improvements are expected to be made beyond the state of the art in the near future and also explaining what technologies have to be developed to reach this performance level.

3.2.1. Sources of Factorizable Photon Pairs

As explained, efficient photon-pair sources have been realized in the LNOI platform using periodically poled ridge waveguides,^[99,104,105] but not engineered for factorizable pair generation. It has been shown theoretically that by a careful design of the width and height of the waveguide and its poling period, factorizable pairs can be generated on the LNOI platform,^[111] where the required sub-micron cross-section of the waveguide and the few-micron poling periods are compatible with current LNOI fabrication capabilities.^[56,70] The design in^[111] results in highly factorizable pairs, with Schmidt numbers down to $K = 1.05$, where K indicates the effective number of entangled pairs of spectral modes, with the ideal factorizable case being $K = 1$. Assuming a common exponential decay in the probability of the entangled spectral modes,^[205] one can calculate the maximum achievable fidelity,^[203] where $K = 1.05$ will result in $F > 0.97$, meaning that the heralding detection has little effect on the quantum state of the single-photon output. This could be further improved by engineering the poling pattern in the waveguide, where an effective Gaussian nonlinearity pattern can result in a near-unity K .^[206] Here, the role of nanostructuring in reaching the required modal dispersion for factorizability should be emphasized, as the dispersion of weakly-guided modes in conventional LN waveguides does not allow for this effect, unless under a counterpropagating pair generation configuration with sub-micron poling periods.^[207] It should also be mentioned, that if the signal and idler have the same central wavelength, as designed in,^[111] the factorizability condition requires that they be in different modes, for example, in the TE and TM modes of the waveguide.^[111] By a proper choice of

the poling period, the design could also be extended to produce signal and idler at different wavelengths. Overall, we can conclude that the source on this platform imposes no fundamental limit on the fidelity of the single-photon output. It should still be noted, that the indistinguishability between the single photons produced from the different sources relies on the fact that all the photon-pair sources are fabricated and poled identical to one another, and it should be investigated to what extent the required tolerances can be met on the LNOI platform. Nevertheless, the electro-optic tuning of individual sources could be thought of as a way of fine-tune the many different sources into indistinguishability with one another.

3.2.2. Pump Rejection Filter and Other Beam Separations

After the photon-pair generation by SPDC, the strong classical pump beam has to be filtered, so that it does not interfere with single photon detection, and the signal and idler photons should be separated from each other. For such passive manipulation, LNOI can borrow solutions from the more matured silicon platform.^[5,208] In general, on-chip pump rejection is a challenging task in all integrated platforms, as the pump has to be filtered with an extinction ratio exceeding 100 dB. We believe that the LNOI platform could facilitate this, mainly because the pump wavelength for SPDC can be very different than the signal and idler (e.g., with the pump in the visible range and the photon pairs in the NIR). To contrast, in pair generation through SFWM the pump wavelength is usually very close to that of the generated photon pairs, making a large-extinction pump rejection, while introducing little loss in the signal and idler channels, very challenging.^[209] We believe that partially effective solutions demonstrated on the silicon platform, such as using Bragg grating filters,^[210,211] can be adapted to the LNOI platform, where the advantage of having a very different pump wavelength could result in a much better filtering performance. Bragg filters have already been implemented on the LNOI platform,^[139] with 25 dB extinction over a 3 nm spectral bandwidth using a 250 μm long periodic Bragg waveguide. Hence, a 1 mm long Bragg filter should give the desired 100 dB extinction, assuming the structure does not suffer from propagation losses outside the photonic bandgap of the Bragg structure. The performance of this particular implementation was limited by the very large 76 dB cm^{-1} propagation losses. This could be improved with the currently available LNOI fabrication technology, which can reach Q-factors above 1 million for photonic crystal resonators,^[212] where a corresponding propagation loss well below 1 dB cm^{-1} can be estimated for the 1D periodic waveguides that constitute these types of resonators.^[213] It should be mentioned that such photonic crystals were implemented for NIR operation, whereas we want to filter a pump in the visible range, which requires a shorter periodicity for the Bragg structure and could potentially make the fabrication more susceptible to scattering-induced losses. However, it has already been shown that nanostructured LNOI elements for visible regime operation can be fabricated with very high qualities comparable to the ones fabricated for NIR operations.^[55] Hence, with the state of the art LNOI fabrication technology, it should be

possible to realize a 1 mm long Bragg filter, that could suppress the visible pump by more than 100 dB and introduce a loss below 0.1 dB for the propagating signal and idler modes in the NIR. We note that the depth of the corrugations in the Bragg waveguide will determine the spectral bandwidth of the photonic bandgap and hence the filter, and should be chosen correspondingly to cover the spectral bandwidth of the pump pulse that is used for generating factorizable photon pairs.

For separation of signal and idler photons of different wavelength or polarization, directional couplers made of two coupled waveguides can be used, which have already been designed and implemented on the LNOI platform,^[136,214] with 10 s of micrometers in coupling length and sub-micron gap separation. Directional couplers can in principle be made to not have any inherent excess losses, if no sharp bends or strong tapers are introduced, and the total loss is determined by the propagation loss of the waveguides that constitute the coupler.^[5] For LNOI ridge waveguides, bending radii in the order of a few 10 s of micrometers are suggested to avoid bending losses.^[137,214,215] We take a total length of around 200 μm for the directional coupler, including bending and coupling regions, as an estimation of the length needed for having a low-loss directional coupler. In addition it should be mentioned, that the pump pulse could be separated into equal channels for feeding the many sources on the chip, which could be done in a compact way using a cascaded Y-splitter tree, as was already demonstrated on the LNOI platform.^[55] The Y-splitters introduce extra losses for the pump, however this only affects the efficiency of the HSPSPs, which could be offset by more pump power or longer sources, and does not affect the fidelity of the single-photon output.

3.2.3. Single-Photon Detectors

To detect single photons for heralding, SNSPDs integrated on waveguide structures can be used.^[172] Such threshold SNSPDs have been implemented recently on ridge waveguides on the LNOI platform with detection efficiencies close to 50%,^[173] although the measured efficiencies in this work was highly underestimated, as the measured value was not corrected for photon losses occurring on-chip between the input port and the SNSPD. It can be expected that the SNSPDs on the LNOI platform could soon reach the common efficiencies of above 90% that is already reached in other integrated platforms.^[172] Using periodic nanobeam structures, near-unity detection efficiencies with recovery times below 10 ns has been reached on other platforms,^[216] which in principle can also be implemented on the LNOI platform, allowing for fast repetition rates for the source. Overall, such threshold detectors have a low sub-100 ps latency in their response,^[217] which lowers the length-requirement for delay lines. For number-resolving capability, transition-edge sensors can be used, which have already been implemented on the conventional titanium in-diffused LN waveguides.^[218] However, such detectors have a very long response time, in the range of few microseconds, which makes them unsuitable for such fast multiplexing applications. For achieving a fast photon-number-resolving response, multiple threshold SNSPDs can be multiplexed together.^[219] Such schemes have a probabilistic

response, where more detectors are needed for a more accurate number-resolving measurement. Nevertheless, high detection efficiencies of 86% have also been reported for such detector systems.^[220] In principle, all such highly efficient on-chip detectors can also be implemented on the LNOI platform.

3.2.4. 2×2 Switches

To perform switching on the single photon output, low loss, and high bandwidth modulators are needed with CMOS compatible driving voltages, which have already been implemented on the LNOI platform.^[86] In ref. [86], a modulator is realized of two parallel 2 cm long ridge waveguides in a Mach-Zehnder interferometer (MZI) configuration with traveling-wave electrodes, with a half-wave voltage of 1.4 V. The modulator has a bandwidth of more than 45 GHz for the applied electrical signals to the electrodes, which allows it to react to very fast sub-nanosecond electrical pulses. Such a modulator can be turned into a 2×2 switch, by substituting the splitter at its beginning and the combiner at its end with 50:50 directional couplers, as shown in Figure 5. Given the fast responses of the LNOI modulators, the repetition rate of the multiplexed source will likely be only limited by the repetition rate of the electronics or the recovery time of the SNSPDs. The demonstrated modulator in ref. [86] has a loss of around 0.5 dB, which is limited by the propagation loss of around 0.2 dB cm^{-1} in the structure. State of the art fabrication of LNOI waveguides has resulted in propagation losses as low as 0.027 dB cm^{-1} .^[13,56,221] For the 2×2 switch, assuming two 200 μm long directional couplers at the beginning and the end of the 2 cm long modulated structure, the total loss of the switch with the state-of-the-art technology could be as low as $2.4 \times 0.027 \approx 0.065 \text{ dB}$. It should be noted, that at cryogenic temperatures the electro-optic coefficient of LN is lowered. Different values have been reported for the increase in the required modulation voltage, such as around 50% increase in ref. [222] and around 10% increase in ref. [223], both at the temperature of 0.8 K and in a modulator based on titanium in-diffused LN waveguides. This effect has been recently measured with an electro-optic switch on the LNOI platform at a temperature of 1.3 K, and an increase of about 15% was measured for the needed modulation voltage compared to room temperature.^[168] At the same time, the cryogenic operation allows the use of superconducting electrodes, which reduce the RF losses in the electrodes, and has been reported to increase the performance of LN modulators,^[224] and could potentially be used to counteract the reduction in the electro-optic coefficient. It was also shown on the LNOI platform, that more novel electrode configurations and designs can improve the performance of the modulator even further.^[154,155]

3.2.5. Electronic Signal Processing and Delay Lines

A crucial step toward a successful implementation of on-chip multiplexing schemes, or in general any type of feed-forward quantum operation,^[225] is the realization of high-repetition rate and low-latency electronics and their integration close to the optical chip.^[5] Latency in this context refers to the delay

between the time a photon hits an SNSPD until the time the processed electrical signal activates the respective switches. During this time, the corresponding single photon in the other channel has to be delayed, to only arrive at the switch after the electrical signal has reached it. An effective way for introducing delay on chip is using a long waveguide,^[226] where a longer delay requires a longer waveguide, which is accompanied by a larger propagation loss. For every 1 ns of on-chip delay an LNOI ridge waveguide of around 14 cm is needed,^[157] which with the best fabrication technology for LNOI results in a loss of around $0.027 \times 14 = 0.378 \text{ dB}$. Hence, every nanosecond of delay to compensate for electronic latency inflicts 0.4 dB of losses on the single-photon output.

All current implementations of multiplexing schemes have electronic latency in the order of hundreds of nanoseconds,^[118] which forces them all to use off-chip optical fibers as a practical solution for introducing such a long delay,^[227–232] where 20 m of fiber is needed to introduce around 100 ns delay. A large part of the electronic latency is caused by the time the radio frequency (RF) signals need to propagate from the detectors to an off-chip circuit for analysis and back to the switch. Having all the optical components on the same chip, which is possible on the LNOI platform, allows for bringing the electronic and optical components close to each other, for example by flip-chip bonding the electronic chip to the optical chip,^[233] which then significantly shortens the communication delay between the optical and the electronic chips. There would still be a latency associated to the processing of electrical signals, which should be minimized as much as possible, using fast and low latency RF and electronic components. Importantly, such components should also be compatible to the cryogenic temperatures, that are necessary for the operation of the SNSPDs. There is active research ongoing toward the development of electronic and RF components for application in quantum technologies,^[234–239] and their review is beyond the scope of this work. Nevertheless, it is important that the existing technology in this area can be optimized for the use in multiplexing applications, to minimize the electronic latency as much as possible, preferably to below a nanosecond.

3.3. Quantifying the Overall Performance of a Spatially Multiplexed Single-Photon Source

Overall, we can conclude that in the LNOI platform, the only constraint on the performance of a spatially multiplexed source of single photons is imposed by the underlying propagation loss of the waveguides, which ultimately limits the probability of having a single photon at the output. To quantify this, let us consider the case of a spatially multiplexed source with threshold SNSPD detectors, as shown schematically in Figure 5. Here we use the methods presented in refs. [118,203,204], which quantify the performance of multiplexed sources under the effect of imperfect components. We simplify our calculations by assuming that the sources can produce perfectly factorizable pairs (which is expected to be possible on the LNOI platform based on the presented discussions) and ignore the dark counts of the detectors, which is a good starting approximation for SNSPD detectors. The effect of both parameters

can be introduced in the calculations based on the methods presented in refs. [118,203,204]. We expect that a detection efficiency above 80% can be realized on the LNOI platform in the near future. In this case, for reaching a fidelity of $F = 0.99$ and an output probability of $P > 0.99$ (assuming no losses yet) a few hundreds of sources need to be multiplexed (692 for 80% detection efficiency and 458 for 100% detection efficiency^[118,203]).

The number of needed HSPSs will have an effect on the number of the switches that will appear in the path of the single photon toward the output. To direct the output of N sources into one output, $N - 1 \times 2 \times 2$ switches are needed, where one way of arranging them is in a log-tree configuration, with the maximum depth of the switching network being $\left\lceil \frac{\ln N}{\ln 2} \right\rceil$.^[204] That means for any number of sources in the range of $513 < N < 1024$ the switching network would have a depth of $\left\lceil \frac{\ln N}{\ln 2} \right\rceil = 10$, meaning that a maximum of 10 switches would appear in the path of a single photon before it reaches the output. Hence, our total switch-induced losses can be estimated to be $0.065 \times 10 = 0.65$ dB.

We now add the loss we expect from the shorter components. We estimated the loss of the pump rejection filter to be around 0.1 dB. The total length of the source depends on the spectral bandwidth that is desired for the generated photons, where a longer source results in a narrower bandwidth and at the same time a more efficient interaction. Here we assume that the source and the separator of the signal and idler have an overall length of 1 cm, which gives a total loss of 0.027 dB, assuming that the single photon could also be lost at any stage in the source. Hence, the overall loss in the path of the single photon output, not considering the delay lines, will be $0.027 + 0.1 + 0.65 = 0.777$ dB. Assuming at least 1 ns of latency in the electronics, the loss introduced by the delay line should be added to this, putting the total loss at $0.777 + 0.378 = 1.155$ dB. This loss corresponds to a probability factor of $10^{-0.1155} \approx 0.77$ for the output signal photon to be present in the output, which lowers the output probability by the same factor, resulting in $P = 0.99 \times 0.77 \approx 0.76$. Overall, the probability that the multiplexed source outputs a triggered single-photon has the lower bound of $q = F \times P = 0.99 \times 0.76 \approx 0.75$.^[204] Compensating each extra nanosecond of latency by adding more delay lines lowers this probability by a factor of $10^{-0.0378} \approx 0.92$. The output probability considering 1 ns latency, surpasses the minimum value of $q = 0.67$, found in ref. [196] as a necessary condition to be met to perform efficient linear optical quantum computation. More specifically, ref. [196] requires the availability of both efficient sources and detectors, where the multiplication of their efficiencies surpass $2/3$. For this condition to be met even with an ideal detector, the source output probability must surpass $2/3$.

3.4. Suggested Paths toward Improvements and Applicability

To improve this generation efficiency and reduce the losses in the presented multiplexed source few paths exists. As discussed, the latency in the electronics should be decreased as much as possible, to reduce the need for delay lines. Even

assuming that future improvement in the fabrication technology on the LNOI platform could reduce the propagation losses significantly and allow for using low-loss few-meter-long delay lines, it has to be noticed that longer delay lines require a larger footprint^[157,240] and fitting many of them on the same substrate might not be feasible. Nevertheless, with the existing technology, reducing the electronic latency to 1 ns is a must, and lowering it even further will reduce the delay-dependent losses. Another path to be followed is the development of fast and efficient number-resolving detectors on the LNOI platform by multiplexing multiple SNSPDs together. To reach this goal, first the efficiency of the single SNSPD detectors on the LNOI platform has to be increased to reach the near-unity efficiency that can be achieved on other platforms, although this goal is expected to be naturally reached in the near-future, considering the current slope of the developments. With number-resolving detectors, the needed number of HSPSs can be reduced from a few hundreds to a few tens of HSPSs. In this case, the depth of the switching network could be reduced by a factor of two, which then reduces the switch-induced losses by a factor of two. It should be mentioned that such detectors should not be truly number resolving, but only be able to distinguish between one photon and more than one photon. It could also be that the reduced number of sources could improve the speed of logical operations in the electronics, as with fewer sources there are fewer logical operations to be done, thereby reducing the total latency and consequently the delay-induced losses.

Finally, we shortly discuss the applicability of this implementation on chip in terms of the footprint the components require. Low-loss LNOI components have been fabricated on a wafer scale on 6-inch LNOI wafers.^[53] Hence, it is in principle possible to fabricate a large number of LNOI components on the same chip. The most spacious components are the switches and the delay lines. For each switch we assume a lateral size of 50 μm , based on optimized designs on the LNOI platform,^[89] which is mostly occupied by the electrodes. Assuming around 700 switches (corresponding to the case of having about 700 HSPSs), given that each switch is about 2.4 cm long, the total footprint needed for the switches is about $700 \times 2.4 \text{ cm} \times 50 \mu\text{m} = 8.4 \text{ cm}^2$. For the delay lines, we assume a lateral size of about a few micrometers, considering the lateral spacing needed between adjacent waveguides to avoid unwanted couplings. With a latency in the order of a few nanoseconds, delay lines with a few tens of centimeters in length are needed, which could potentially be formed into curved or spiral shapes for an economic fitting.^[157] Hence, each delay line is about an order of magnitude longer and about an order of magnitude narrower in lateral size compared to a switch, which overall means that the delay lines occupy about the same footprint as the switches. The rest of the components put together are much shorter in length compared to the switches and the delay lines and consequently require much less footprint. From this discussion, we can estimate that all the optical components need a footprint in the order of 20 cm^2 , which fits well within the area of a 6-inch wafer. It should be noted, that this is an estimate of the minimum needed footprint. To reach this minimum footprint, the components have to be properly arranged on the chip. In this arrangement, the feasibility of connection to the electronic chip through flip-chip bonding should also be taken into account.

3.5. A Short Discussion on Other Quantum Optical Applications Based on Similar Circuitry on LNOI

In our discussion on multiplexing, we mainly focused on the application of the LNOI platform for discrete-variable (DV) quantum simulation and computation,^[1,3] which are based on using single photon states. There exist also continuous-variable (CV) protocols, based on using squeezed states in the high gain regime of pair generation, which have attracted interest due to avoiding some of the practical complexities of the DV approaches.^[2,241–243] Low-confinement integrated LN waveguides have already gained attraction for implementation of CV operations,^[244] due to their high efficiency in generation of squeezed states,^[245] which is expected to be even more efficient on the high-confinement LNOI platform.^[246] There are also hybrid DV and CV approaches for quantum information processing,^[247,248] where the LNOI platform could be particularly useful for their on-chip implementation.

Specifically, a similar circuit structure as shown in Figure 5 can also be used for a fully on-chip implementation of quantum simulation based on Gaussian Boson sampling (GBS),^[242,243] with the difference that photon-pair sources should be replaced by sources of squeezed light with spectral factorizability. Preliminary calculations have suggested that squeezing factors of 20 dB could be possible using state-of-the-art LNOI ridge waveguides.^[246] As said, factorizability is also reachable on this platform. The 2×2 switches can be used to create a reconfigurable interference network between the squeezed outputs for performing a unitary operation and reprogramming the circuit for different simulations. Fast feed-forwarding and hence delay lines would not be required here. The single-photon detectors would be moved to the end of the circuit, where number-resolving capability is needed for this application, which as said is in principle possible on LNOI. The filters would be needed to reject the pump. The directional couplers are needed to separate the signal and idler. We clearly see the utility of LNOI for different fully on-chip optical quantum circuits, where the analysis we presented for multiplexed single-photon sources can similarly be extended to evaluate their performance.

4. Conclusion

In this perspective, we tried to promote the notion that LNOI is a platform which is very well suited for the realization of integrated quantum photonics on large scales. As we showed, basically all elements needed to realize quantum-optic functionalities have been already implemented and experimentally characterized, albeit usually in classical contexts. However, based on these elements, quantum circuits comparable to recent demonstrations in silicon photonics can be implemented in a straightforward manner. However, as we detailed in the section on the implementation of a single photon source, LNOI enables to go even further and at least potentially enables the implementation of such sources which are of central importance especially for applications in photonic quantum computing. Based on our analysis, we are convinced that lithium niobate, one of the classical materials of integrated and nonlinear optics, has a bright future also for integrated quantum photonics.

Acknowledgements

The authors acknowledge funding from the German Federal Ministry of Education and Research (BMBF) under the project identifier 13N14877 (QuanIm4Life) and from the German Research Foundation (DFG) under the project identifier 407070005 (NanoPair), SE 2749/1-1 (NanoSPDC), 398816777-SFB 1375 (NOA), and from the Thuringian Ministry for Economic Affairs, Science and Digital Society under the project identifier 2021 FGI 0043 (Quantum Hub Thuringia) and 2017IZN 0012 (InQuoSens) as well as from the German Academic Exchange Service (DAAD) under the project identifier 57448581 (PPP Taiwan 2019).

Open access funding enabled and organized by Projekt DEAL.

Conflict of Interest

The authors declare no conflict of interest.

Keywords

integrated optics, lithium niobate, photonic integrated circuits, quantum circuits, quantum photonics

Received: April 18, 2021

Revised: June 20, 2021

Published online: September 12, 2021

- [1] F. Flamini, N. Spagnolo, F. Sciarrino, *Rep. Prog. Phys.* **2018**, *82*, 016001.
- [2] D. J. Brod, E. F. Galvão, A. Crespi, R. Osellame, N. Spagnolo, *Adv. Photonics* **2019**, *1*, 034001.
- [3] S. Slussarenko, G. J. Pryde, *Appl. Phys. Rev.* **2019**, *6*, 4.
- [4] J. Wang, F. Sciarrino, A. Laing, M. G. Thompson, *Nat. Photonics* **2020**, *14*, 273.
- [5] J. C. Adcock, J. Bao, Y. Chi, X. Chen, D. Bacco, Q. Gong, L. K. Oxenlowe, J. Wang, Y. Ding, *IEEE J. Sel. Top. Quantum Electron.* **2020**, *27*, 6700224.
- [6] S. Bogdanov, M. Shalaginov, A. Boltasseva, V. M. Shalaev, *Opt. Mater. Express* **2017**, *7*, 111.
- [7] A. W. Elshaari, W. Pernice, K. Srinivasan, O. Benson, V. Zwiller, *Nat. Photonics* **2020**, *14*, 285.
- [8] O. Alibart, V. D'Auria, M. D. Micheli, F. Doutré, F. Kaiser, L. Labonté, T. Lunghi, É. Picholle, S. Tanzilli, *J. Opt.* **2016**, *18*, 10.
- [9] G. Poberaj, H. Hu, W. Sohler, P. Guenter, *Laser Photonics Rev.* **2012**, *6*, 488.
- [10] A. Boes, B. Corcoran, L. Chang, J. Bowers, A. Mitchell, *Laser Photonics Rev.* **2018**, *12*, 1700256.
- [11] A. Honardoost, K. Abdelsalam, S. Fathpour, *Laser Photonics Rev.* **2020**, *14*, 2000088.
- [12] Y. Qi, Y. Li, *Nanophotonics* **2020**, *9*, 1287.
- [13] J. Lin, F. Bo, Y. Cheng, J. Xu, *Photonics Res.* **2020**, *8*, 1910.
- [14] Y. Zheng, X. Chen, *Adv. Phys.: X* **2021**, *6*, 1889402.
- [15] Y. Jia, L. Wang, F. Chen, *Appl. Phys. Rev.* **2021**, *8*, 011307.
- [16] D. Zhu, L. Shao, M. Yu, R. Cheng, B. Desiatov, C. J. Xin, Y. Hu, J. Holzgrafe, S. Ghosh, A. Shams-Ansari, E. Puma, N. Sinclair, C. Reimer, M. Zhang, M. Lonär, *arXiv:2102.11956*, **2021**.
- [17] M. Reig Escalé, F. Kaufmann, H. Jiang, D. Pohl, R. Grange, *APL Photonics* **2020**, *5*, 121301.
- [18] M. Yu, L. Shao, Y. Okawachi, A. L. Gaeta, M. Loncar, in *CLEO: Science and Innovations*, Optical Society of America, Washington, D.C. **2020**, STu4H-1.
- [19] T. Jin, J. Zhou, P. T. Lin, *Sci. Rep.* **2019**, *9*, 15130.

- [20] W. Yue, Y. Ding, B. Wu, Y. Shen, *Opt. Lett.* **2020**, *45*, 383.
- [21] Y. M. Sua, H. Fan, A. Shahverdi, J.-Y. Chen, Y.-P. Huang, *Sci. Rep.* **2017**, *7*, 17494.
- [22] A. Solntsev, P. Kumar, T. Pertsch, A. Sukhorukov, F. Setzpfandt, *APL Photonics* **2018**, *3*, 2.
- [23] M. Armenise, *IEE Proc. J (Optoelectron.)* **1988**, *135*, 85.
- [24] W. Sohler, H. Hu, R. Ricken, V. Quiring, C. Vannahme, H. Herrmann, D. Büchter, S. Reza, W. Grundkötter, S. Orlov, H. Suche, R. Nouroozi, Y. Min, *Opt. Photonics News* **2008**, *19*, 24.
- [25] M. De Micheli, J. Botineau, P. Sibillot, D. Ostrowsky, M. Papuchon, *Opt. Commun.* **1982**, *42*, 101.
- [26] S. Tanzilli, A. Martin, F. Kaiser, M. P. de Micheli, O. Alibart, D. B. Ostrowsky, *Laser Photonics Rev.* **2012**, *6*, 115.
- [27] A. Solntsev, F. Setzpfandt, A. Clark, C. Wu, M. Collins, C. Xiong, A. Schreiber, F. Katzschmann, F. Eilenberger, R. Schiek, W. Sohler, A. Mitchell, C. Silberhorn, B. Eggleton, T. Pertsch, A. Sukhorukov, D. Neshev, Y. Kivshar, *Phys. Rev. X* **2014**, *4*, 3.
- [28] H. Jin, F. Liu, P. Xu, J. Xia, M. Zhong, Y. Yuan, J. Zhou, Y. Gong, W. Wang, S. Zhu, *Phys. Rev. Lett.* **2014**, *113*, 103601.
- [29] P. Sharapova, K. Luo, H. Herrmann, M. Reichelt, T. Meier, C. Silberhorn, *New J. Phys.* **2017**, *19*, 123009.
- [30] K.-H. Luo, S. Brauner, C. Eigner, P. R. Sharapova, R. Ricken, T. Meier, H. Herrmann, C. Silberhorn, *Sci. Adv.* **2019**, *5*, eaat1451.
- [31] F. Setzpfandt, A. S. Solntsev, J. Titchener, C. W. Wu, C. Xiong, R. Schiek, T. Pertsch, D. N. Neshev, A. A. Sukhorukov, *Laser Photonics Rev.* **2015**, *10*, 131.
- [32] J. Wang, S. Paesani, Y. Ding, R. Santagati, P. Skrzypczyk, A. Salavrakos, J. Tura, R. Augusiak, L. Mančinska, D. Bacco, D. Bonneau, J. W. Silverstone, Q. Gong, A. Acín, K. Rottwitt, L. K. Oxenløwe, J. L. O'Brien, A. Laing, M. G. Thompson, *Science* **2018**, *360*, 285.
- [33] X. Qiang, X. Zhou, J. Wang, C. M. Wilkes, T. Loke, S. O'Gara, L. Kling, G. D. Marshall, R. Santagati, T. C. Ralph, D. Bonneau, J. W. Silverstone, Q. Gong, A. Acín, K. Rottwitt, L. K. Oxenløwe, J. L. O'Brien, A. Laing, M. G. Thompson, *Nat. Photonics* **2018**, *12*, 534.
- [34] F. Schrepel, T. Gischkat, H. Hartung, E. B. Kley, W. Wesch, *Nucl. Instrum. Methods Phys. Res., Sect. B* **2006**, *250*, 164.
- [35] H. Hartung, E.-B. Kley, A. Tünnermann, T. Gischkat, F. Schrepel, W. Wesch, *Opt. Lett.* **2008**, *33*, 2320.
- [36] R. Geiss, S. Diziain, R. Iliew, C. Etrich, H. Hartung, N. Janunts, F. Schrepel, F. Lederer, T. Pertsch, E. B. Kley, *Appl. Phys. Lett.* **2010**, *97*, 131109.
- [37] S. Diziain, R. Geiss, M. Zilk, F. Schrepel, E. B. Kley, A. Tünnermann, T. Pertsch, *Appl. Phys. Lett.* **2013**, *103*, 051117.
- [38] M. Levy, R. M. Osgood, R. Liu, L. E. Cross, G. S. Cargill, A. Kumar, H. Bakhrui, *Appl. Phys. Lett.* **1998**, *73*, 2293.
- [39] P. Rabiei, P. Gunter, *Appl. Phys. Lett.* **2004**, *85*, 4603.
- [40] H. Han, L. Cai, H. Hu, *Opt. Mater.* **2015**, *42*, 47.
- [41] L. Cai, S. L. H. Han, H. Hu, *Opt. Express* **2015**, *23*, 1240.
- [42] N. Courjal, B. Guichardaz, G. Ulliac, J.-Y. Rauch, B. Sadani, H.-H. Lu, M.-P. Bernal, *J. Phys. D: Appl. Phys.* **2011**, *44*, 305101.
- [43] R. Takigawa, E. Higurashi, T. Kawanishi, T. Asano, *Opt. Express* **2014**, *22*, 27733.
- [44] M. F. Volk, S. Suntsov, C. E. Rüter, D. Kip, *Opt. Express* **2016**, *24*, 1386.
- [45] R. Geiss, S. Saravi, A. Sergeyev, S. Diziain, F. Setzpfandt, F. Schrepel, R. Grange, E.-B. Kley, A. Tünnermann, T. Pertsch, *Opt. Lett.* **2015**, *40*, 12.
- [46] S. Diziain, R. Geiss, M. Steinert, C. Schmidt, W.-K. Chang, S. Fasold, D. Fülßel, Y.-H. Chen, T. Pertsch, *Opt. Mater. Express* **2015**, *5*, 2081.
- [47] J. Lin, Y. Xu, Z. Fang, M. Wang, J. Song, N. Wang, L. Qiao, W. Fang, Y. Cheng, *Sci. Rep.* **2015**, *5*, 8072.
- [48] R. Wu, J. Zhang, N. Yao, W. Fang, L. Qiao, Z. Chai, J. Lin, Y. Cheng, *Opt. Lett.* **2018**, *43*, 4116.
- [49] P. Rabiei, W. H. Steier, *Appl. Phys. Lett.* **2005**, *86*, 161115.
- [50] H. Hu, R. Ricken, W. Sohler, *Opt. Express* **2009**, *17*, 24261.
- [51] A. Guarino, G. Poberaj, D. Rezzonico, R. Degl'Innocenti, P. Günter, *Nat. Photonics* **2007**, *1*, 407.
- [52] L. Chang, Y. Li, N. Volet, L. Wang, J. Peters, J. E. Bowers, *Optica* **2016**, *3*, 531.
- [53] K. Luke, P. Kharel, C. Reimer, L. He, M. Loncar, M. Zhang, *Opt. Express* **2020**, *28*, 24452.
- [54] C. Wang, C. Langrock, A. Marandi, M. Jankowski, M. Zhang, B. Desiatov, M. M. Fejer, M. Lončar, *Optica* **2018**, *5*, 1438.
- [55] B. Desiatov, A. Shams-Ansari, M. Zhang, C. Wang, M. Lončar, *Optica* **2019**, *6*, 380.
- [56] M. Zhang, C. Wang, R. Cheng, A. Shams-Ansari, M. Lončar, *Optica* **2017**, *4*, 1536.
- [57] M. Li, J. Ling, Y. He, U. A. Javid, S. Xue, Q. Lin, *Nat. Commun.* **2020**, *11*, 4123.
- [58] L. Cai, H. Han, S. Zhang, H. Hu, K. Wang, *Opt. Lett.* **2014**, *39*, 2094.
- [59] H. Liang, R. Luo, Y. He, H. Jiang, Q. Lin, *Optica* **2017**, *4*, 1251.
- [60] H. Jiang, H. Liang, R. Luo, X. Chen, Y. Chen, Q. Lin, *Appl. Phys. Lett.* **2018**, *113*, 021104.
- [61] M. Li, H. Liang, R. Luo, Y. He, Q. Lin, *Laser Photonics Rev.* **2019**, *13*, 5.
- [62] A. Fedotova, M. Younesi, J. Sautter, A. Vaskin, F. J. Löchner, M. Steinert, R. Geiss, T. Pertsch, I. Staude, F. Setzpfandt, *Nano Lett.* **2020**, *20*, 8608.
- [63] J. Ma, F. Xie, W. Chen, J. Chen, W. Wu, W. Liu, Y. Chen, W. Cai, M. Ren, J. Xu, *Laser Photonics Rev.* **2021**, *15*, 2000521.
- [64] L. Carletti, A. Zilli, F. Moia, A. Toma, M. Finazzi, C. De Angelis, D. N. Neshev, M. Celebrano, *ACS Photonics* **2021**, *8*, 731.
- [65] T. Santiago-Cruz, A. Fedotova, V. Sultanov, M. A. Weissflog, D. Arslan, M. Younesi, T. Pertsch, I. Staude, F. Setzpfandt, M. V. Chekhova, *arXiv:2103.08524*, **2021**.
- [66] S. Saravi, T. Pertsch, F. Setzpfandt, *Phys. Rev. Lett.* **2017**, *118*, 18.
- [67] S. Saravi, T. Pertsch, F. Setzpfandt, *Opt. Lett.* **2019**, *44*, 69.
- [68] V. Y. Shur, A. R. Akhmatkhanov, I. S. Baturin, *Appl. Phys. Rev.* **2015**, *2*, 040604.
- [69] P. Mackwitz, M. Rüsing, G. Berth, A. Widhalm, K. Müller, A. Zrenner, *Appl. Phys. Lett.* **2016**, *108*, 152902.
- [70] J. Zhao, M. Rüsing, M. Roeper, L. M. Eng, S. Mookherjea, *J. Appl. Phys.* **2020**, *127*, 193104.
- [71] J. T. Nagy, R. M. Reano, *Opt. Mater. Express* **2020**, *10*, 1911.
- [72] M. Younesi, R. Geiss, S. Rajaei, F. Setzpfandt, Y.-H. Chen, T. Pertsch, *J. Opt. Soc. Am. B* **2021**, *38*, 685.
- [73] J.-C. Duan, J.-N. Zhang, Y.-J. Zhu, C.-W. Sun, Y.-C. Liu, P. Xu, Z. Xie, Y.-X. Gong, S.-N. Zhu, *J. Opt. Soc. Am. B* **2020**, *37*, 2139.
- [74] A. Rao, K. Abdelsalam, T. Sjaardema, A. Honardoost, G. F. Camacho-Gonzalez, S. Fathpour, *Opt. Express* **2019**, *27*, 25920.
- [75] J. Zhao, M. Rüsing, U. A. Javid, J. Ling, M. Li, Q. Lin, S. Mookherjea, *Opt. Express* **2020**, *28*, 19669.
- [76] J. Lu, J. B. Surya, X. Liu, A. W. Bruch, Z. Gong, Y. Xu, H. X. Tang, *Optica* **2019**, *6*, 1455.
- [77] R. Wolf, I. Breunig, H. Zappe, K. Buse, *Opt. Express* **2017**, *25*, 29927.
- [78] D. Wang, T. Ding, Y. Zheng, X. Chen, *Opt. Express* **2019**, *27*, 15283.
- [79] M. Yu, B. Desiatov, Y. Okawachi, A. L. Gaeta, M. Lončar, *Opt. Lett.* **2019**, *44*, 1222.
- [80] Z. Gong, X. Liu, Y. Xu, M. Xu, J. B. Surya, J. Lu, A. Bruch, C. Zou, H. X. Tang, *Opt. Lett.* **2019**, *44*, 3182.
- [81] M. Zhang, B. Buscaino, C. Wang, A. Shams-Ansari, C. Reimer, R. Zhu, J. M. Kahn, M. Lončar, *Nature* **2019**, *568*, 373.
- [82] C. Wang, M. Zhang, M. Yu, R. Zhu, H. Hu, M. Loncar, *Nat. Commun.* **2019**, *10*, 978.

- [83] Z. Gong, X. Liu, Y. Xu, H. X. Tang, *Optica* **2020**, 7, 1275.
- [84] L. Shao, M. Yu, S. Maity, N. Sinclair, L. Zheng, C. Chia, A. Shams-Ansari, C. Wang, M. Zhang, K. Lai, M. Lončar, *Optica* **2019**, 6, 1498.
- [85] H. Jiang, X. Yan, H. Liang, R. Luo, X. Chen, Y. Chen, Q. Lin, *Appl. Phys. Lett.* **2020**, 117, 081102.
- [86] C. Wang, M. Zhang, X. Chen, M. Bertrand, A. Shams-Ansari, S. Chandrasekhar, P. Winzer, M. Lončar, *Nature* **2018**, 562, 101.
- [87] P. O. Weigel, J. Zhao, K. Fang, H. Al-Rubaye, D. Trotter, D. Hood, J. Mudrick, C. Dallo, A. T. Pomerene, A. L. Starbuck, C. T. DeRose, A. L. Lentine, G. Rebeiz, S. Mookherjea, *Opt. Express* **2018**, 26, 23728.
- [88] X. Wang, P. O. Weigel, J. Zhao, M. Ruesing, S. Mookherjea, *APL Photonics* **2019**, 4, 096101.
- [89] A. Honardoost, F. A. Juneghani, R. Safian, S. Fathpour, *Opt. Express* **2019**, 27, 6495.
- [90] D. Bonneau, J. W. Silverstone, M. G. Thompson, in *Silicon Photonics III* (eds: L. Pavesi, D. J. Lockwood), Springer, Berlin, Heidelberg **2016**, pp. 41–82.
- [91] D. J. Blumenthal, R. Heideman, D. Geuzebroek, A. Leinse, C. Roeloffzen, *Proc. IEEE* **2018**, 106, 2209.
- [92] C. P. Dietrich, A. Fiore, M. G. Thompson, M. Kamp, S. Höfling, *Laser Photonics Rev.* **2016**, 10, 870.
- [93] D. C. Burnham, D. L. Weinberg, *Phys. Rev. Lett.* **1970**, 25, 84.
- [94] K.-i. Harada, H. Takesue, H. Fukuda, T. Tsuchizawa, T. Watanabe, K. Yamada, Y. Tokura, S.-i. Itabashi, *Opt. Express* **2008**, 16, 20368.
- [95] E. Engin, D. Bonneau, C. M. Natarajan, A. S. Clark, M. G. Tanner, R. H. Hadfield, S. N. Dorenbos, V. Zwiller, K. Ohira, N. Suzuki, H. Yoshida, N. Iizuka, M. Ezaki, J. L. O'Brien, M. G. Thompson, *Opt. Express* **2013**, 21, 27826.
- [96] P. Imany, J. A. Jaramillo-Villegas, O. D. Odele, K. Han, D. E. Leaird, J. M. Lukens, P. Lougovski, M. Qi, A. M. Weiner, *Opt. Express* **2018**, 26, 1825.
- [97] X. Lu, Q. Li, D. A. Westly, G. Moille, A. Singh, V. Anant, K. Srinivasan, *Nat. Phys.* **2019**, 15, 373.
- [98] I. W. Frank, J. Moore, J. K. Douglas, R. Camacho, M. Eichenfield, in *2016 Conference on Lasers and Electro-Optics, CLEO 2016*, Optical Society of America, Washington, D.C. **2016**, SM2E.6.
- [99] R. Luo, H. Jiang, S. Rogers, H. Liang, Y. He, Q. Lin, *Opt. Express* **2017**, 25, 24531.
- [100] Z. Ma, J.-Y. Chen, Z. Li, C. Tang, Y. M. Sua, H. Fan, Y.-P. Huang, *Phys. Rev. Lett.* **2020**, 125, 263602.
- [101] J. Zhao, C. Ma, M. Rüsing, S. Mookherjea, *Phys. Rev. Lett.* **2020**, 124, 163603.
- [102] J.-Y. Chen, Y. M. Sua, Z.-H. Ma, C. Tang, Z. Li, Y.-p. Huang, *OSA Continuum* **2019**, 2, 2914.
- [103] B. S. Elkus, K. Abdelsalam, A. Rao, V. Velez, S. Fathpour, P. Kumar, G. S. Kanter, *Opt. Express* **2019**, 27, 38521.
- [104] G.-T. Xue, Y.-F. Niu, X. Liu, J.-C. Duan, W. Chen, Y. Pan, K. Jia, X. Wang, H.-Y. Liu, Y. Zhang, P. Xu, G. Zhao, X. Cai, Y.-X. Gong, X. Hu[‡], Z. Xie, S. Zhu, *arXiv:2012.06092*, **2020**.
- [105] U. A. Javid, J. Ling, J. Staffa, M. Li, Y. He, Q. Lin, *arXiv:2101.04877*, **2021**.
- [106] B. S. Elkus, K. Abdelsalam, S. Fathpour, P. Kumar, G. S. Kanter, *Opt. Express* **2020**, 28, 39963.
- [107] C. Ma, X. Wang, V. Anant, A. D. Beyer, M. D. Shaw, S. Mookherjea, *Opt. Express* **2017**, 25, 32995.
- [108] C. Xiong, C. Monat, A. S. Clark, C. Grillet, G. D. Marshall, M. J. Steel, J. Li, L. O'Faolain, T. F. Krauss, J. G. Rarity, B. J. Eggleton, *Opt. Lett.* **2011**, 36, 3413.
- [109] D. Kang, A. Pang, Y. Zhao, A. S. Helmy, *J. Opt. Soc. Am. B* **2014**, 31, 1581.
- [110] M. Gilaberte Basset, F. Setzpfandt, F. Steinlechner, E. Beckert, T. Pertsch, M. Gräfe, *Laser Photonics Rev.* **2019**, 13, 10.
- [111] S. Paesani, Y. Ding, R. Santagati, L. Chakhmakhchyan, C. Vigliar, K. Rottwitt, L. K. Oxenløwe, J. Wang, M. G. Thompson, A. Laing, *Nat. Phys.* **2019**, 15, 925.
- [112] E. Knill, R. Laflamme, G. J. Milburn, *Nature* **2001**, 409, 46.
- [113] S. Fasel, O. Alibart, S. Tanzilli, P. Baldi, A. Beveratos, N. Gisin, H. Zbinden, *New J. Phys.* **2004**, 6, 163.
- [114] S. Cappelletto, R. Scholten, *The Eur. Phys. J. Appl. Phys.* **2008**, 41, 181.
- [115] S. Signorini, L. Pavesi, *AVS Quantum Sci.* **2020**, 2, 041701.
- [116] E. Meyer-Scott, C. Silberhorn, A. Migdall, *Rev. Sci. Instrum.* **2020**, 91, 041101.
- [117] M. D. Eisaman, J. Fan, A. Migdall, S. V. Polyakov, *Rev. Sci. Instrum.* **2011**, 82, 071101.
- [118] S. Dutta, E. A. Goldschmidt, S. Barik, U. Saha, E. Waks, *Nano Lett.* **2020**, 20, 741.
- [119] S. Wang, L. Yang, R. Cheng, Y. Xu, M. Shen, R. L. Cone, C. W. Thiel, H. X. Tang, *Appl. Phys. Lett.* **2020**, 116, 151103.
- [120] Q. Luo, Z. Hao, C. Yang, R. Zhang, D. Zheng, S. Liu, H. Liu, F. Bo, Y. Kong, G. Zhang, J. Xu, *Sci. China Phys., Mechan., Astron.* **2021**, 64, 234263.
- [121] Z. Chen, Q. Xu, K. Zhang, W.-H. Wong, D.-L. Zhang, E. Y.-B. Pun, C. Wang, *Opt. Lett.* **2021**, 46, 1161.
- [122] J. Zhou, Y. Liang, Z. Liu, W. Chu, H. Zhang, D. Yin, Z. Fang, R. Wu, J. Zhang, W. Chen, Z. Wang, Y. Zhou, M. Wang, Y. Cheng, *arXiv:2101.00783*, **2021**.
- [123] Z. Wang, Z. Fang, Z. Liu, W. Chu, Y. Zhou, J. Zhang, R. Wu, M. Wang, T. Lu, Y. Cheng, *Opt. Lett.* **2021**, 46, 380.
- [124] Y. Liu, X. Yan, J. Wu, B. Zhu, Y. Chen, X. Chen, *Sci. China Phys., Mechan., Astron.* **2021**, 64, 234262.
- [125] D. Pak, H. An, A. Nandi, X. Jiang, Y. Xuan, M. Hosseini, *J. Appl. Phys.* **2020**, 128, 084302.
- [126] K. Xia, F. Sardi, C. Sauerzapf, T. Kornher, H.-W. Becker, Z. Kis, L. Kovacs, R. Kolesov, J. Wrachtrup, *arXiv:2104.00389*, **2021**.
- [127] S. Aghaeimeibodi, B. Desiatov, J. H. Kim, C. M. Lee, M. A. Buyukkaya, A. Karasahin, C. J. Richardson, R. P. Leavitt, M. Lončar, E. Waks, *Appl. Phys. Lett.* **2018**, 113, 221102.
- [128] R. Loudon, P. L. Knight, *J. Mod. Opt.* **1987**, 34, 709.
- [129] D. Serkland, P. Kumar, M. Arbore, M. Fejer, *Opt. Lett.* **1997**, 22, 1497.
- [130] G. S. Kanter, P. Kumar, R. V. Roussev, J. Kurz, K. R. Parameswaran, M. M. Fejer, *Opt. Express* **2002**, 10, 177.
- [131] K.-i. Yoshino, T. Aoki, A. Furusawa, *Appl. Phys. Lett.* **2007**, 90, 041111.
- [132] J. Lu, A. A. Sayem, Z. Gong, J. B. Surya, C.-L. Zou, H. X. Tang, *arXiv:2101.04735*, **2021**.
- [133] M. Prost, G. Liu, S. B. Yoo, in *2018 Optical Fiber Communications Conference and Exposition (OFC)*, IEEE, Piscataway, NJ **2018**, pp. 1–3.
- [134] C. Wang, M. Zhang, B. Stern, M. Lipson, M. Lončar, *Opt. Express* **2018**, 26, 1547.
- [135] X. Li, M. Wang, J. Li, K. Chen, *IEEE Photonics Technol. Lett.* **2019**, 31, 1611.
- [136] Z. Gong, W. Ji, R. Yin, J. Li, Z. Song, *IEEE Photonics Technol. Lett.* **2020**, 32, 787.
- [137] H. Xu, D. Dai, L. Liu, Y. Shi, *Opt. Express* **2020**, 28, 10899.
- [138] J. Schollhammer, M. A. Baghban, K. Gallo, *Opt. Lett.* **2017**, 42, 3578.
- [139] M. A. Baghban, J. Schollhammer, C. Errando-Herranz, K. B. Gylfason, K. Gallo, *Opt. Express* **2017**, 25, 32323.
- [140] M. R. Escalé, D. Pohl, A. Sergeev, R. Grange, *Opt. Lett.* **2018**, 43, 1515.
- [141] A. Prencipe, M. A. Baghban, K. Gallo, in *Integrated Photonics Research, Silicon and Nanophotonics*, Optical Society of America, Washington, D.C. **2020**, pp. IW2A–5.
- [142] J. R. Ong, R. Kumar, S. Mookherjea, *IEEE Photonics Technol. Lett.* **2013**, 25, 1543.
- [143] M. Piekarek, D. Bonneau, S. Miki, T. Yamashita, M. Fujiwara, M. Sasaki, H. Terai, M. G. Tanner, C. M. Natarajan, R. H. Hadfield, J. L. O'Brien, M. G. Thompson, *Opt. Lett.* **2017**, 42, 815.

- [144] J. Lu, M. Li, C.-L. Zou, A. Al Sayem, H. X. Tang, *Optica* **2020**, *7*, 1654.
- [145] T. Pertsch, R. Iwanow, R. Schiek, G. Stegeman, U. Peschel, F. Lederer, Y. H. Min, W. Sohler, *Opt. Lett.* **2005**, *30*, 177.
- [146] X. Liu, X. Zhong, P. Ying, J. Xu, Y. Han, S. Yu, X. Cai, *Opt. Lett.* **2020**, *45*, 6318.
- [147] M. Xu, M. He, H. Zhang, J. Jian, Y. Pan, X. Liu, L. Chen, X. Meng, H. Chen, Z. Li, X. Xiao, S. Yu, S. Yu, X. Cai, *Nat. Commun.* **2020**, *11*, 3911.
- [148] J. Wang, F. Bo, S. Wan, W. Li, F. Gao, J. Li, G. Zhang, J. Xu, *Opt. Express* **2015**, *23*, 23072.
- [149] C. Wang, M. Zhang, B. Stern, M. Lipson, M. Lončar, *Opt. Express* **2018**, *26*, 1547.
- [150] L. Cai, Y. Kang, H. Hu, *Opt. Express* **2016**, *24*, 4640.
- [151] T. Ren, M. Zhang, C. Wang, L. Shao, C. Reimer, Y. Zhang, O. King, R. Esman, T. Cullen, M. Loncar, *IEEE Photonics Technol. Lett.* **2019**, *31*, 889.
- [152] D. Pohl, A. Messner, F. Kaufmann, M. R. Escalé, J. Holzer, J. Leuthold, R. Grange, *IEEE Photonics Technol. Lett.* **2020**, *33*, 85.
- [153] A. Prencipe, M. A. Baghban, K. Gallo, *arXiv:2103.06831*, **2021**.
- [154] P. Kharel, C. Reimer, K. Luke, L. He, M. Zhang, *Optica* **2021**, *8*, 357.
- [155] M. Jin, J. Chen, Y. Sua, P. Kumar, Y. Huang, *Opt. Lett.* **2021**, *46*, 1884.
- [156] M. Jin, J.-Y. Chen, Y. M. Sua, Y.-P. Huang, *Opt. Lett.* **2019**, *44*, 1265.
- [157] J. X. Zhou, R. H. Gao, J. Lin, M. Wang, W. Chu, W. B. Li, D. F. Yin, L. Deng, Z. W. Fang, J. H. Zhang, R. B. Wu, Y. Cheng, *Chin. Phys. Lett.* **2020**, *37*, 084201.
- [158] R. Wu, J. Lin, M. Wang, Z. Fang, W. Chu, J. Zhang, J. Zhou, Y. Cheng, *Opt. Lett.* **2019**, *44*, 4698.
- [159] M. Zhang, K. Chen, M. Wang, J. Wu, K. S. Chiang, *Opt. Lett.* **2021**, *46*, 1001.
- [160] M. Wang, N. Yao, R. Wu, Z. Fang, S. Lv, J. Zhang, J. Lin, W. Fang, Y. Cheng, *New J. Phys.* **2020**, *22*, 073030.
- [161] P. Kumar, *Opt. Lett.* **1990**, *15*, 1476.
- [162] H. Fan, Z. Ma, J. Chen, Z. Li, C. Tang, Y. Sua, Y. Huang, *arXiv:2102.07044*, **2021**.
- [163] M. Kues, C. Reimer, J. M. Lukens, W. J. Munro, A. M. Weiner, D. J. Moss, R. Morandotti, *Nat. Photonics* **2019**, *13*, 170.
- [164] Y. Hu, M. Yu, D. Zhu, N. Sinclair, A. Shams-Ansari, L. Shao, J. Holzgrafe, E. Puma, M. Zhang, M. Loncar, *arXiv:2005.09621*, **2020**.
- [165] T. Ding, X. Chen, Y. Zheng, *J. Lightwave Technol.*, Vol. 37, Issue 4, pp. 1296-1300 **2019**, *37*, 1296.
- [166] J. Wu, Y. Huang, C. Lu, T. Ding, Y. Zheng, X. Chen, *Phys. Rev. Appl.* **2020**, *13*, 064068.
- [167] M. Zhang, C. Wang, Y. Hu, A. Shams-Ansari, T. Ren, S. Fan, M. Lončar, *Nat. Photonics* **2019**, *13*, 36.
- [168] E. Lomonte, M. A. Wolff, F. Beutel, S. Ferrari, C. Schuck, W. H. Pernice, F. Lenzini, *arXiv:2103.10973*, **2021**.
- [169] B. Desiatov, M. Lončar, *Appl. Phys. Lett.* **2019**, *115*, 121108.
- [170] E. Saglamyurek, N. Sinclair, J. Jin, J. A. Slater, D. Oblak, F. Bussières, M. George, R. Ricken, W. Sohler, W. Tittel, *Nature* **2011**, *469*, 512.
- [171] I. Esmail Zadeh, J. W. Los, R. B. Gourgues, V. Steinmetz, G. Bulgarini, S. M. Dobrovolskiy, V. Zwiller, S. N. Dorenbos, *APL Photonics* **2017**, *2*, 111301.
- [172] S. Ferrari, C. Schuck, W. Pernice, *Nanophotonics* **2018**, *7*, 1725.
- [173] A. A. Sayem, R. Cheng, S. Wang, H. X. Tang, *Appl. Phys. Lett.* **2020**, *116*, 151102.
- [174] M. Colangelo, B. Desiatov, D. Zhu, J. Holzgrafe, O. Medeiros, M. Loncar, K. K. Berggren, in *Conference on Lasers and Electro-Optics (2020)*, Optical Society of America, Washington, D.C. **2020**, p. SM4O.4
- [175] J. Wang, D. Bonneau, M. Villa, J. W. Silverstone, R. Santagati, S. Miki, T. Yamashita, M. Fujiwara, M. Sasaki, H. Terai, M. G. Tanner, C. M. Natarajan, R. H. Hadfield, J. L. O'Brien, M. G. Thompson, *Optica* **2016**, *3*, 407.
- [176] D. Llewellyn, Y. Ding, I. I. Faruque, S. Paesani, D. Bacco, R. Santagati, Y.-J. Qian, Y. Li, Y.-F. Xiao, M. Huber, M. Malik, G. F. Sinclair, X. Zhou, K. Rottwitz, J. L. O'Brien, J. G. Rarity, Q. Gong, L. K. Oxenlowe, J. Wang, M. G. Thompson, *Nat. Phys.* **2020**, *16*, 148.
- [177] Z. Chen, R. Peng, Y. Wang, H. Zhu, H. Hu, *Opt. Mater. Express* **2017**, *7*, 4010.
- [178] I. Krasnokutskaya, R. J. Chapman, J.-L. J. Tambasco, A. Peruzzo, *Opt. Express* **2019**, *27*, 17681.
- [179] K. Shuting, ru Zhang, Z. Hao, J. Di, F. Gao, F. Bo, G. Zhang, J. Xu, *Opt. Lett.* **2020**, *45*, 6651.
- [180] S. Yang, Y. Li, J. Xu, M. Wang, L. Wu, X. Quan, M. Liu, L. Fu, X. Cheng, *Opt. Mater. Express* **2021**, *11*, 1366.
- [181] J. Cardenas, C. B. Poitras, K. Luke, L.-W. Luo, P. A. Morton, M. Lipson, *IEEE Photonics Technol. Lett.* **2014**, *26*, 2380.
- [182] L. He, M. Zhang, A. Shams-Ansari, R. Zhu, C. Wang, L. Marko, *Opt. Lett.* **2019**, *44*, 2314.
- [183] N. Yao, J. Zhou, R. Gao, J. Lin, M. Wang, Y. Cheng, W. Fang, L. Tong, *Opt. Express* **2020**, *28*, 12416.
- [184] I. Krasnokutskaya, J.-L. J. Tambasco, A. Peruzzo, *Opt. Express* **2019**, *27*, 16578.
- [185] C. Hu, A. Pan, T. Li, X. Wang, Y. Liu, S. Tao, C. Zeng, J. Xia, *Opt. Express* **2021**, *29*, 5397.
- [186] P. Ying, H. Tan, J. Zhang, M. He, M. Xu, X. Liu, R. Ge, Y. Zhu, C. Liu, X. Cai, *Opt. Lett.* **2021**, *46*, 1478.
- [187] P. O. Weigel, M. Savanier, C. T. DeRose, A. T. Pomerene, A. L. Starbuck, A. L. Lentine, V. Stenger, S. Mookherjea, *Sci. Rep.* **2016**, *6*, 22301.
- [188] M. Rusing, P. O. Weigel, J. Zhao, S. Mookherjea, *IEEE Nano-technol. Mag.* **2019**, *13*, 18.
- [189] L. Chang, M. H. Pfeiffer, N. Volet, M. Zervas, J. D. Peters, C. L. Manganelli, E. J. Stanton, Y. Li, T. J. Kippenberg, J. E. Bowers, *Opt. Lett.* **2017**, *42*, 803.
- [190] A. N. R. Ahmed, A. Mercante, S. Shi, P. Yao, D. W. Prather, *Opt. Lett.* **2018**, *43*, 4140.
- [191] A. N. R. Ahmed, S. Shi, M. Zabolocki, P. Yao, D. W. Prather, *Opt. Lett.* **2019**, *44*, 618.
- [192] W. Jiang, C. J. Sarabalis, Y. D. Dahmani, R. N. Patel, F. M. Mayor, T. P. McKenna, R. Van Laer, A. H. Safavi-Naeini, *Nat. Commun.* **2020**, *11*, 1.
- [193] J. Holzgrafe, N. Sinclair, D. Zhu, A. Shams-Ansari, M. Colangelo, Y. Hu, M. Zhang, K. K. Berggren, M. Lončar, *Optica* **2020**, *7*, 1714.
- [194] T. P. McKenna, J. D. Witmer, R. N. Patel, W. Jiang, R. V. Laer, P. Arrangoiz-Arriola, E. A. Wollack, J. F. Herrmann, A. H. Safavi-Naeini, *Optica* **2020**, *7*, 1737.
- [195] M. A. Nielsen, *Phys. Rev. Lett.* **2004**, *93*, 040503.
- [196] M. Varnava, D. E. Browne, T. Rudolph, *Phys. Rev. Lett.* **2008**, *100*, 060502.
- [197] M. Gimeno-Segovia, P. Shadbolt, D. E. Browne, T. Rudolph, *Phys. Rev. Lett.* **2015**, *115*, 020502.
- [198] Y. Li, P. C. Humphreys, G. J. Mendoza, S. C. Benjamin, *Phys. Rev. X* **2015**, *5*, 041007.
- [199] G.-B. Xu, Q.-Y. Wen, F. Gao, S.-J. Qin, *Quantum Inf. Process.* **2014**, *13*, 2587.
- [200] J. Wang, Q. Zhang, C.-j. Tang, *Opt. Commun.* **2006**, *266*, 732.
- [201] M. Pant, H. Krovi, D. Englund, S. Guha, *Phys. Rev. A* **2017**, *95*, 012304.
- [202] A. L. Migdall, D. Branning, S. Castelletto, *Phys. Rev. A* **2002**, *66*, 053805.
- [203] A. Christ, C. Silberhorn, *Phys. Rev. A* **2012**, *85*, 023829.
- [204] D. Bonneau, G. J. Mendoza, J. L. O'Brien, M. G. Thompson, *New J. Phys.* **2015**, *17*, 043057.

- [205] A. Christ, K. Laiho, A. Eckstein, K. N. Cassemiro, C. Silberhorn, *New J. Phys.* **2011**, *13*, 033027.
- [206] A. M. Brańczyk, A. Fedrizzi, T. M. Stace, T. C. Ralph, A. G. White, *Opt. Express* **2011**, *19*, 55.
- [207] A. Christ, A. Eckstein, P. J. Mosley, C. Silberhorn, *Opt. Express* **2009**, *17*, 3441.
- [208] J. W. Silverstone, J. Wang, D. Bonneau, P. Sibson, R. Santagati, C. Erven, J. O'Brien, M. Thompson, in *2016 International Conference on Optical MEMS and Nanophotonics (OMN)*, IEEE, Piscataway, NJ **2016**, pp. 1–2.
- [209] R. R. Kumar, X. Wu, H. K. Tsang, *Opt. Lett.* **2020**, *45*, 1289.
- [210] N. C. Harris, D. Grassani, A. Simbula, M. Pant, M. Galli, T. Baehr-Jones, M. Hochberg, D. Englund, D. Bajoni, C. Galland, *Phys. Rev. X* **2014**, *4*, 041047.
- [211] D. Oser, F. Mazeas, X. Le Roux, D. Pérez-Galacho, O. Alibart, S. Tanzilli, L. Labonté, D. Marris-Morini, L. Vivien, É. Cassan, C. Alonso-Ramos, *Laser Photonics Rev.* **2019**, *13*, 1800226.
- [212] M. Li, H. Liang, R. Luo, Y. He, J. Ling, Q. Lin, *Optica* **2019**, *6*, 860.
- [213] J. D. Witmer, J. A. Valery, P. Arrangoiz-Arriola, C. J. Sarabalis, J. T. Hill, A. H. Safavi-Naeini, *Sci. Rep.* **2017**, *7*, 46313.
- [214] Z. Gong, R. Yin, W. Ji, J. Wang, C. Wu, X. Li, S. Zhang, *Opt. Commun.* **2017**, *396*, 23.
- [215] L. Zhang, X. Fu, L. Yang, *Appl. Opt.* **2020**, *59*, 8668.
- [216] M. K. Akhlaghi, E. Schelew, J. F. Young, *Nat. Commun.* **2015**, *6*, 8233.
- [217] J. P. Allmaras, A. G. Kozorezov, B. A. Korzh, K. K. Berggren, M. D. Shaw, *Phys. Rev. Appl.* **2019**, *11*, 034062.
- [218] J. P. Höpker, T. Gerrits, A. Lita, S. Krapick, H. Herrmann, R. Ricken, V. Quiring, R. Mirin, S. W. Nam, C. Silberhorn, T. J. Bartley, *APL Photonics* **2019**, *4*, 056103.
- [219] F. Mattioli, Z. Zhou, A. Gaggero, R. Gaudio, S. Jahanmirinejad, D. Sahin, F. Marsili, R. Leoni, A. Fiore, *Supercond. Sci. Technol.* **2015**, *28*, 104001.
- [220] M. Moshkova, A. Divochiy, P. Morozov, Y. Vakhtomin, A. Antipov, P. Zolotov, V. Seleznev, M. Ahmetov, K. Smirnov, *J. Opt. Soc. Am. B* **2019**, *36*, B20.
- [221] R. Wu, M. Wang, J. Xu, J. Qi, W. Chu, Z. Fang, J. Zhang, J. Zhou, L. Qiao, Z. Chai, J. Lin, Y. Cheng, *Nanomaterials* **2018**, *8*, 910.
- [222] F. Thiele, F. Vom Bruch, V. Quiring, R. Ricken, H. Herrmann, C. Eigner, C. Silberhorn, T. J. Bartley, *Opt. Express* **2020**, *28*, 28961.
- [223] A. Youssefi, I. Shomroni, Y. J. Joshi, N. Bernier, A. Lukashchuk, P. Urich, L. Qiu, T. J. Kippenberg, *arXiv:2004.04705*, **2020**.
- [224] K. Yoshida, Y. Kanda, S. Kohjiro, *IEEE Trans. Microwave Theor. Tech.* **1999**, *47*, 1201.
- [225] R. Prevedel, P. Walther, F. Tiefenbacher, P. Böhi, R. Kaltenbaek, T. Jennewein, A. Zeilinger, *Nature* **2007**, *445*, 65.
- [226] L. Zhou, X. Wang, L. Lu, J. Chen, *Chin. Opt. Lett.* **2018**, *16*, 101301.
- [227] M. J. Collins, C. Xiong, I. H. Rey, T. D. Vo, J. He, S. Shahnian, C. Reardon, T. F. Krauss, M. J. Steel, A. S. Clark, B. J. Eggleton, *Nat. Commun.* **2013**, *4*, 2582.
- [228] T. Meany, L. A. Ngah, M. J. Collins, A. S. Clark, R. J. Williams, B. J. Eggleton, M. Steel, M. J. Withford, O. Alibart, S. Tanzilli, *Laser Photonics Rev.* **2014**, *8*, L42.
- [229] T. Kiyohara, R. Okamoto, S. Takeuchi, *Opt. Express* **2016**, *24*, 27288.
- [230] G. J. Mendoza, R. Santagati, J. Munns, E. Hemsley, M. Piekarek, E. Martín-López, G. D. Marshall, D. Bonneau, M. G. Thompson, J. L. O'Brien, *Optica* **2016**, *3*, 127.
- [231] M. G. Puigibert, G. Aguilar, Q. Zhou, F. Marsili, M. Shaw, V. Verma, S. Nam, D. Oblak, W. Tittel, *Phys. Rev. Lett.* **2017**, *119*, 083601.
- [232] F. Kaneda, P. G. Kwiat, *Sci. Adv.* **2019**, *5*, eaaw8586.
- [233] N. Pavarelli, J. S. Lee, M. Rensing, C. Scarcella, S. Zhou, P. Ossieur, P. A. O'Brien, *J. Lightwave Technol.* **2015**, *33*, 991.
- [234] J. M. Hornibrook, J. I. Colless, I. D. Conway Lamb, S. J. Pauka, H. Lu, A. C. Gossard, J. D. Watson, G. C. Gardner, S. Fallahi, M. J. Manfra, D. J. Reilly, *Phys. Rev. Appl.* **2015**, *3*, 024010.
- [235] I. Conway Lamb, J. Colless, J. Hornibrook, S. Pauka, S. Waddy, M. Frechtling, D. Reilly, *Rev. Sci. Instrum.* **2016**, *87*, 014701.
- [236] H. Homulle, S. Visser, B. Patra, G. Ferrari, E. Prati, F. Sebastiano, E. Charbon, *Rev. Sci. Instrum.* **2017**, *88*, 045103.
- [237] C. Cahall, D. J. Gauthier, J. Kim, *Rev. Sci. Instrum.* **2018**, *89*, 063117.
- [238] Y. Salathé, P. Kurpiers, T. Karg, C. Lang, C. K. Andersen, A. Akin, S. Krinner, C. Eichler, A. Wallraff, *Phys. Rev. Appl.* **2018**, *9*, 034011.
- [239] J. P. van Dijk, E. Charbon, F. Sebastiano, *Microprocess. Microsyst.* **2019**, *66*, 90.
- [240] H. Lee, T. Chen, J. Li, O. Painter, K. J. Vahala, *Nat. Commun.* **2012**, *3*, 867.
- [241] N. C. Menicucci, P. Van Loock, M. Gu, C. Weedbrook, T. C. Ralph, M. A. Nielsen, *Phys. Rev. Lett.* **2006**, *97*, 110501.
- [242] C. S. Hamilton, R. Kruse, L. Sansoni, S. Barkhofen, C. Silberhorn, I. Jex, *Phys. Rev. Lett.* **2017**, *119*, 170501.
- [243] J. M. Arrazola, V. Bergholm, K. Brádler, T. R. Bromley, M. J. Collins, I. Dhand, A. Fumagalli, T. Gerrits, A. Goussev, L. G. Helt, J. Hundal, T. Isacsson, R. B. Israel, J. Izaac, S. Jahangiri, R. Janik, N. Killoran, S. P. Kumar, J. Lavoie, A. E. Lita, D. H. Mahler, M. Menotti, B. Morrison, S. W. Nam, L. Neuhaus, H. Y. Qi, N. Quesada, A. Repington, K. K. Sabapathy, M. Schuld, D. Su, J. Swinerton, A. Száva, K. Tan, P. Tan, V. D. Vaidya, Z. Vernon, Z. Zabaneh, Y. Zhang, *Nature* **2021**, *591*, 54.
- [244] F. Lenzini, J. Janousek, O. Thearle, M. Villa, B. Haylock, S. Kasture, L. Cui, H.-P. Phan, D. V. Dao, H. Yonezawa, P. K. Lam, E. H. Huntington, M. Lobino, *Sci. Adv.* **2018**, *4*, eaat9331.
- [245] F. Mondaini, T. Lunghi, A. Zavatta, E. Gouzien, F. Doutre, M. De Micheli, S. Tanzilli, V. D'Auria, *Photonics Res.* **2019**, *7*, A36.
- [246] M. Jankowski, J. Mishra, M. Fejer, *arXiv:2103.02296*, **2021**.
- [247] U. L. Andersen, J. S. Neergaard-Nielsen, P. Van Loock, A. Furusawa, *Nat. Phys.* **2015**, *11*, 713.
- [248] S. Takeda, A. Furusawa, *APL Photonics* **2019**, *4*, 060902.



Sina Saravi is a postdoctoral researcher in the Nano and Quantum Optics group at the Friedrich Schiller University Jena, Germany. He studied electrical engineering at the Iran University of Science and Technology, Tehran, Iran. He received his M.Sc. in photonics and PhD in physics from the Friedrich Schiller University Jena, Germany. His research focuses on nanostructured nonlinear sources of photon pairs, quantum imaging and spectroscopy, as well as the fundamental description of nonlinear quantum-optical interactions at the nanoscale.



Thomas Pertsch is Professor for Applied Physics at the Friedrich Schiller University in Jena, Germany, where he heads the Nano and Quantum Optics group. He studied electrical engineering at the Technical University Dresden, Germany and Rensselaer Polytechnic Institute, Troy, USA. He received his PhD from the Friedrich Schiller University Jena. His research focuses on the generation and ultrafast dynamics of light in nanostructured matter, including metamaterials and photonic crystals as well as on quantum photonics.



Frank Setzpfandt is a research group leader for quantum optics at the Friedrich Schiller University in Jena, Germany. He studied physics at the Friedrich Schiller University, from which he also received his PhD. Before returning to Jena, he spent time as a PostDoc at the Australian National University in Canberra. His research is concentrating on nonlinear frequency conversion and the generation of photon pairs, quantum imaging and sensing, and integrated quantum optics.